JOURNAL OF GUIDANCE, CONTROL, AND DYNAMICS
Vol. 27, No. 3, May–June 2004

Singularity Analysis of Variable-Speed Control Moment Gyros

Hyungjoo Yoon* and Panagiotis Tsiotras†
Georgia Institute of Technology, Atlanta, Georgia 30332-0150

Single-gimbal control moment gyros (CMGs) have many advantages over other actuators for attitude control of spacecraft. For instance, they act as torque amplifiers and, thus, are suitable for slew maneuvers. However, their use as torque actuators is hindered by the presence of singularities, that, when encountered, do not allow a CMG cluster to generate torques about arbitrary directions. One method to overcome this drawback is to use variable-speed single-gimbal control moment gyros (VSCMGs). Whereas the wheel speed of a conventional CMG is constant, VSCMGs are allowed to have variable wheel speed. Therefore, VSCMGs have extra degrees of freedom that can be used to achieve additional objectives, such as singularity avoidance and/or power tracking, as well as attitude control. The singularity problem of a VSCMGs cluster is studied in detail for the cases of attitude tracking, with and without a power tracking requirement. A null motion method to avoid singularities is presented, and a criterion is developed to determine the momentum region over which this method will successfully avoid singularities. This criterion can be used to size the wheels and develop appropriate momentum damping strategies tailored to the specific mission requirements.

I. Introduction

A CONTROL moment gyro (CMG) is a device used as an actuator for attitude control of spacecraft. It generates torques through angular momentum transfer to and from the main spacecraft body. This is achieved by changing the direction of the angular momentum vector of a gimballed flywheel. Because a CMG operates in a continuous manner, contrary to the gas jet's on/off operation, it can achieve precise attitude control. Moreover, as with other momentum exchange devices, for example, reaction wheels, it does not consume any propellant, thus prolonging the operational life of the spacecraft. Single-gimbal CMGs essentially act as torque amplifiers.[1] This torque amplification property makes them especially advantageous as attitude control actuators for large space spacecraft and space structures, for example, a space station. In fact, single-gimbal and double-gimbal CMGs have been used for attitude control of the Skylab, the MIR and the International Space Station (ISS).

An obstacle when using a CMG system in practice is the existence of singular gimbal angle states for which the CMGs cannot generate a torque along arbitrary directions. At each singular state, all admissible torque directions lie on a two-dimensional surface in the three-dimensional angular momentum space; therefore, the CMG system cannot generate a torque normal to this surface. The CMG singularities can be classified into two categories: 1) external or saturated singularities in which the total angular momentum sum of the CMGs lies on the maximum momentum envelope and 2) internal singularities in which the total momentum lies inside this envelope. The external singularities can be easily anticipated from the given CMG configuration and mission profile; therefore, they can be taken into account at the design step. A properly designed momentum management scheme can also relieve the external singularity problem. The internal CMG singularities, on the other hand, are in general difficult to anticipate. Avoiding such internal singularities has, thus, been a long-standing problem in the CMG attitude control literature.[1−3] Various methods have been developed during the last few decades for avoiding CMG singularities, for example, the gradient method with null motion,[1,3,4] the singularity robust methods,[5−8] the path planning method,[9] the preferred gimbal angle method,[10] the workspace restriction method,[4,11] etc.

In the present paper, a singularity avoidance method using single gimbal variable speed CMGs (VSCMGs) is presented. The concept of a VSCMG was first introduced by Ford and Hall,[12] where it was called "gimballed momentum wheel." The term VSCMG was coined in Ref. 13 and emphasizes the fact that these devices typically function as conventional CMGs. Whereas the wheel speed of a conventional CMG is kept constant, the wheel speed of a VSCMG is allowed to vary continuously. Thus, a VSCMG can be considered as a hybrid between a reaction wheel and a conventional CMG. The extra degree of freedom, owing to the wheel speed changes, can be used to avoid the singularities. Also it allows a VSCMG to be used as an actuator in an integrated power/attitude control system (IPACS).[14,15] Such a scheme uses reaction wheels or VSCMGs as "mechanical batteries" to store energy in addition to providing torques for attitude control.

An IPACS combines the energy-storage and the attitude-control functions into a single device, which, thus, increases reliability and significantly reduces the overall weight and spacecraft size. This concept has been studied since the 1960s,[16] but it has become particularly popular during the last decade, thanks to the recent advances in composite materials and magnetic bearing technology. A complete survey of IPACS has been given in Refs. 14 and 17. VSCMGs have been used for attitude control and energy storage for an IPACS in the authors' previous work.[15] In particular, in Ref. 15 the gimbal rates of the VSCMGs were used to provide the reference tracking torques, whereas the wheel accelerations were used both for attitude and power reference tracking. The control algorithm performs both the attitude and power tracking goals simultaneously. However, the singularity problem was not dealt with explicitly in Refs. 15 and 18.

The present paper complements the results of Ref. 15, as well as those of Refs. 19 and 20, in several aspects. First, we provide a mathematical analysis for the singularities of a VSCMG cluster and present a singularity avoidance method using null motion for the VSCMG case. When applied to conventional CMGs, this analysis provides new insights into the issue of CMG singularities. In addition, it is more straightforward than existing ones.[19,21] Second, we offer a singularity avoidance and escape method (using null motion) and we characterize the conditions for its validity. Note that although a singularity avoidance method using VSCMGs, has also been introduced in Ref. 20, conditions are not provided in Ref. 20 under which such a strategy is possible. Moreover, in Ref. 20

Received 7 June 2003; revision received 7 September 2003; accepted for publication 24 October 2003.

*Ph.D. Candidate, School of Aerospace Engineering; hyungjoo_yoon@ae.gatech.edu. Student Member AIAA.

†Associate Professor, School of Aerospace Engineering; p.tsiotras@ae.gatech.edu. Associate Fellow AIAA.

the authors restrict the discussion to the case of attitude tracking, whereas in the present paper we include the case of simultaneous attitude and power tracking. As shown in Sec. VI, this has several important repercussions to the singularity classification and avoidance problem.

This paper is organized as follows: In Sec. II, we provide the equations of a VSCMG actuator. In Sec. III, we define a singularity of a VSCMG cluster and related key terminology for both CMGs and VSCMGs. In Sec. IV, we provide a condition in which null motion can exist at a singular configuration. It is shown that a CMG cluster with no less than two wheels operating in VSCMG mode will avoid all singularities using null motion. A singularity avoidance scheme using null motion and based on the gradient method is also proposed in Sec. V. The analysis includes the case of combined attitude and power constraints, and it is given in Sec. VI. We show that there are singularities for which the null motion method does not work if both attitude and power tracking requirements have to be met simultaneously. In Sec. VII, we provide a geometric analysis on these singular states. As a result of this analysis, in Sec. VIII we present a simple criterion for determining whether such singularities are encountered. Finally, in Sec. IX we present numerical examples for the verification of the singularity analysis and the proposed singularity avoidance method for VSCMGs.

II. System Model

Consider a rigid spacecraft with a cluster of N single-gimbal VSCMGs that are used to produce internal torques onboard a spacecraft. The mutually orthogonal unit vectors of the ith VSCMG are shown in Fig. 1 and are defined as follows:

$\boldsymbol{g}_i$ = gimbal axis vector
$\boldsymbol{s}_i$ = spin axis vector
$\boldsymbol{t}_i$ = transverse axis vector (torque vector), given as $\boldsymbol{g}_i \times \boldsymbol{s}_i$

The wheel of the VSCMG can rotate about the gimbal axis $\boldsymbol{g}_i$ with a gimbal angle γ_i. The wheel can also rotate about the spin axis $\boldsymbol{s}_i$ with an angular speed Ω_i. The unit vectors $\boldsymbol{s}_i$ and $\boldsymbol{t}_i$ depend on the gimbal angle γ_i, while the gimbal axis vector $\boldsymbol{g}_i$ is fixed in the body frame. The relationship between the derivatives of these unit vectors can be written as

$$\dot{\boldsymbol{s}}_i = \dot{\gamma}_i \boldsymbol{t}_i, \qquad \dot{\boldsymbol{t}}_i = -\dot{\gamma}_i \boldsymbol{s}_i, \qquad \dot{\boldsymbol{g}}_i = 0, \qquad i = 1, \ldots, N \quad (1)$$

There are several ways to configure a number of VSCMG units. The standard pyramid configuration with four VSCMG units is emphasized here (Fig. 2). The skew angle θ in Fig. 2 is chosen as $\cos\theta = 1/\sqrt{3}$ ($\theta \approx 54.74$ deg) so that the pyramid becomes half of a regular octahedron. This configuration has been studied extensively because it is only once redundant and its momentum envelope (Sec. III.A) is nearly spherical[7] and three-axis symmetric.[22]

In deriving the equations for a VSCMG actuator, we will assume that the gimbal rates $\dot{\gamma}_i$ are much smaller than the wheel speeds Ω_i,

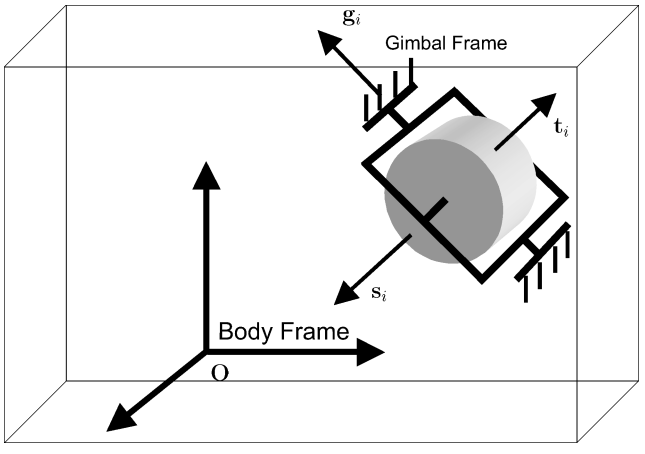

Fig. 1 Spacecraft body with a single VSCMG.

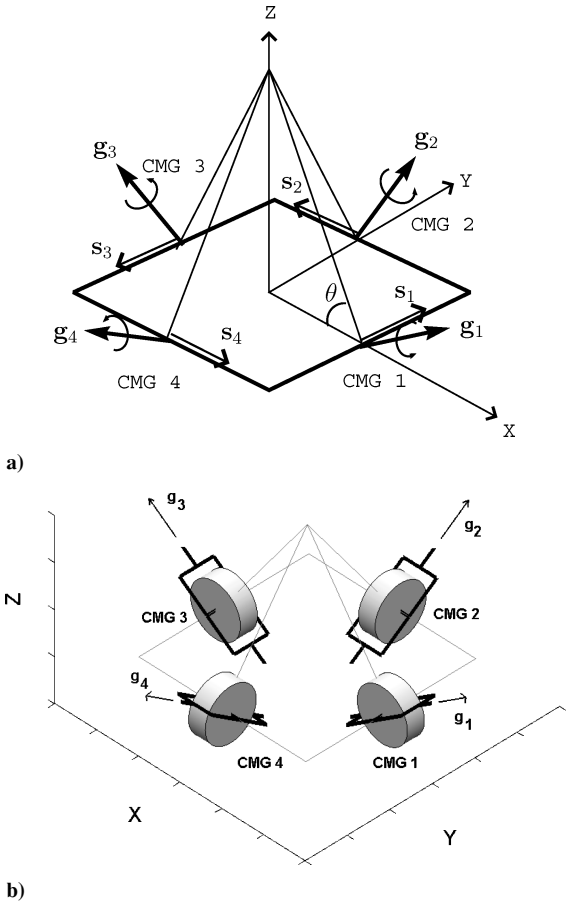

Fig. 2 VSCMG system with pyramid configuration.

so that $\dot{\gamma}_i$ do not contribute to the total angular momentum. We will also neglect the moments of inertia of the gimbal frame structures. These assumptions are common in the studies of CMGs/VSCMGs systems, and they are accurate for typical CMG/spacecraft configurations. For the exact equations of motion of a spacecraft with VSCMG actuators without these assumptions, see Refs. 13 and 15.

With a slight abuse of notation, in the sequel we use bold letters to denote both a vector and its elements in the standard basis. The angular momentum vector of each wheel can be expressed as $h_i \boldsymbol{s}_i$, for $i = 1, \ldots, N$, where $h_i = I_{\mathrm{ws}_i}\Omega_i$ and with I_{ws_i} denoting the moment of inertia of the ith VSCMG wheel about its spin axis. The total angular momentum $\boldsymbol{H}$ of the VSCMG system is the vector sum of the individual momenta of each wheel

$$\boldsymbol{H}(\gamma_1, \ldots, \gamma_N, \Omega_1, \ldots, \Omega_N) = \sum_{i=1}^{N} h_i \boldsymbol{s}_i \quad (2)$$

The time derivative of $\boldsymbol{H}$ is equal to the torque $\boldsymbol{T}$ applied from the spacecraft main body to the VSCMG system, which is equal and opposite to the output torque from the VSCMG to the spacecraft body. This relation is written as

$$\boldsymbol{T} = \dot{\boldsymbol{H}} = \sum_{i=1}^{N} h_i \boldsymbol{t}_i \dot{\gamma}_i + \sum_{i=1}^{N} \boldsymbol{s}_i I_{\mathrm{ws}_i} \dot{\Omega}_i \quad (3)$$

and in matrix form

$$\begin{bmatrix} C(\boldsymbol{\Omega}, \boldsymbol{\gamma}) & D(\boldsymbol{\gamma}) \end{bmatrix} \begin{bmatrix} \dot{\boldsymbol{\gamma}} \\ \dot{\boldsymbol{\Omega}} \end{bmatrix} = \boldsymbol{T} \quad (4)$$

where $C : \mathbb{R}^N \times [0, 2\pi)^N \to \mathbb{R}^{3\times N}$ and $D : [0, 2\pi)^N \to \mathbb{R}^{3\times N}$ are matrix-valued functions given by

$$C(\boldsymbol{\Omega}, \boldsymbol{\gamma}) \triangleq [I_{\mathrm{ws}_1}\Omega_1 \boldsymbol{t}_1, \ldots, I_{\mathrm{ws}_N}\Omega_N \boldsymbol{t}_N] \quad (5)$$

$$D(\boldsymbol{\gamma}) \triangleq [I_{\mathrm{ws}_1}\boldsymbol{s}_1, \ldots, I_{\mathrm{ws}_N}\boldsymbol{s}_N] \quad (6)$$

and where $\gamma \triangleq (\gamma_1, \ldots, \gamma_N)^T \in [0, 2\pi)^N$ and $\Omega \triangleq (\Omega_1, \ldots, \Omega_N)^T \in \mathbb{R}^N$. Notice that Eq. (4) is also valid for a conventional CMG system, if we set the wheel speeds Ω_i to be constant ($\dot{\Omega} = 0$), and for a reaction wheel system, if we set the gimbal angles γ_i to be constant ($\dot{\gamma} = 0$).

III. Singular Configurations of a VSCMGs System

If there are at least two wheels and their (fixed) gimbal axes are not parallel to each other, as in the pyramid configuration, and if none of the wheel speeds becomes zero, the column vectors of $[C \;\; D]$ in Eq. (4) always span the three-dimensional space, that is, rank $([C \;\; D]) = 3$ (Ref. 13). This means that we can always solve Eq. (4) for any given torque command $\boldsymbol{T}$. It follows that such a VSCMG system is always able to generate control torques along an arbitrary direction. In other words, such a VSCMG system never falls into a singularity because of the extra degrees of freedom provided by wheel speed control.[13,15,20] However, the norm of the column vectors of the matrix C is much larger than those of the matrix D. It is, therefore, preferable to generate the required torque using gimbal angle changes, that is, as in CMGs, rather than using wheel speed changes, that is, as in reaction wheels. (This is the torque amplification effect of a CMG, which is the main advantage of the CMG system over other actuators.) Also, for high wheel speeds it is power inefficient to produce torques via wheel acceleration/deceleration. Therefore, in practice, it is desirable to keep rank $C = 3$. In the sequel we define as a singularity of a VSCMG cluster the rank deficiency of the matrix C, even though the VSCMGs will be able to generate an arbitrary torque at such cases. Notice that if none of the wheel speeds is zero, the matrix C defined in Eq. (5) becomes singular if and only if the unit vectors $\boldsymbol{t}_i$ span a two-dimensional plane, similarly to the conventional CMG case. Hence, the rank of the matrix $C(\Omega, \gamma)$ in Eq. (5) is independent of the (nonzero) wheel speeds. This observation leads us to the conclusion that the singularities of VSCMGs occur at a similar condition as the singularities of the conventional CMGs. Before the analysis of singularities of VSCMGs is continued, it is, therefore, imperative to review briefly the singularities of conventional CMGs. This will also allow the introduction of the key terminology that is essential in the ensuing analysis of VSCMGs.

A. Brief Review of the Singularities of a CMG System

For simplicity, and without loss of generality, let us assume that $h_i = 1$ for $i = 1, \ldots, N$. Then the torque equation (4) becomes

$$C(\gamma)\dot{\gamma} = \boldsymbol{T} \tag{7}$$

where $C(\gamma) = [\boldsymbol{t}_1, \ldots, \boldsymbol{t}_N]$. To generate a torque $\boldsymbol{T}$ along an arbitrary direction, we need rank $C(\gamma) = 3$ for all $\gamma \in [0, 2\pi)^N$. If rank $C(\gamma_s) \neq 3$ for some γ_s, however, $\dot{\gamma}$ cannot be calculated for arbitrary torque commands. [Even in this case, there may exist a solution $\dot{\gamma}$ to Eq. (7), if the required torque $\boldsymbol{T}$ lies in the two-dimensional range of $C(\gamma_s)$, but this can be treated as an exceptional case.] Thus, henceforth we define the singularities of a CMG system as the gimbal states γ_s for which rank $C(\gamma_s) = 2$. (Rank $C = 1$ can happen only in very special configuration, for example, in roof-type configuration,[4] and so we neglect this case.) In the singular states all unit vectors $\boldsymbol{t}_i$ lie on the same plane, and thus, we can define a singular direction vector $\boldsymbol{u}$ that is normal to this plane, that is,

$$\boldsymbol{u}^T \boldsymbol{t}_i = 0, \qquad \forall i = 1, \ldots, N \tag{8}$$

Moreover, $\boldsymbol{t}_i$ is normal to $\boldsymbol{g}_i$ by definition, so that $\boldsymbol{t}_i$ is normal to the plane spanned by $\boldsymbol{g}_i$ and $\boldsymbol{u}$. Geometrically this means that each $\boldsymbol{s}_i$ has a maximal or minimal (negatively maximal) projection onto the singular vector $\boldsymbol{u}$, that is, the dot product $\boldsymbol{u} \cdot \boldsymbol{s}_i$ is maximal or minimal,[1] as shown in Fig. 3.

For a given singular vector $\boldsymbol{u} \neq \pm \boldsymbol{g}_i$, there are two possibilities:

$$\boldsymbol{u} \cdot \boldsymbol{t}_i = 0, \qquad \boldsymbol{u} \cdot \boldsymbol{s}_i > 0, \quad \text{or} \quad \boldsymbol{u} \cdot \boldsymbol{t}_i = 0, \qquad \boldsymbol{u} \cdot \boldsymbol{s}_i < 0 \tag{9}$$

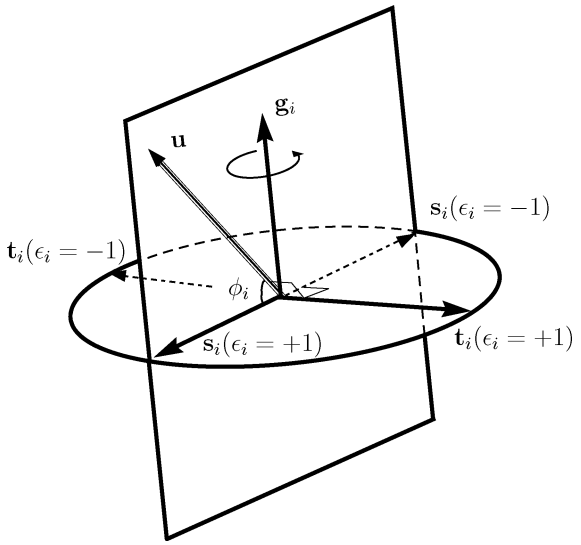

Fig. 3 Vectors at a singular gimbal state.

When $\epsilon_i \triangleq \text{sign}(\boldsymbol{u} \cdot \boldsymbol{s}_i)$ is defined, the torque axis vector and the spin axis vector at a singular state can be obtained as

$$\boldsymbol{t}_i = \epsilon_i \boldsymbol{g}_i \times \boldsymbol{u} / |\boldsymbol{g}_i \times \boldsymbol{u}|, \qquad \boldsymbol{u} \neq \pm \boldsymbol{g}_i, \qquad i = 1, \ldots, N \tag{10}$$

$$\boldsymbol{s}_i = \boldsymbol{t}_i \times \boldsymbol{g}_i = \epsilon_i (\boldsymbol{g}_i \times \boldsymbol{u}) \times \boldsymbol{g}_i / |\boldsymbol{g}_i \times \boldsymbol{u}|, \qquad \boldsymbol{u} \neq \pm \boldsymbol{g}_i \qquad i = 1, \ldots, N \tag{11}$$

and therefore, the total angular momentum at the singular states corresponding to a singular direction $\boldsymbol{u}$ is expressed as[1,4,19]

$$\boldsymbol{H} = \sum_{i=1}^{N} \boldsymbol{s}_i = \sum_{i=1}^{N} \epsilon_i (\boldsymbol{g}_i \times \boldsymbol{u}) \times \frac{\boldsymbol{g}_i}{|\boldsymbol{g}_i \times \boldsymbol{u}|}, \qquad \boldsymbol{u} \neq \pm \boldsymbol{g}_i \tag{12}$$

Hence, given a set of ϵ_i, we can draw a singular surface, which is defined as the locus of the total momentum vector at the singular states, for all $\boldsymbol{u} \in \mathbb{R}^3$ with $\|\boldsymbol{u}\| = 1$, $\boldsymbol{u} \neq \pm \boldsymbol{g}_i$, where $\| \cdot \|$ denotes the Euclidian norm. Figure 4 shows examples of these singular surfaces for a pyramid configuration for two different combinations of $\epsilon_1, \epsilon_2, \epsilon_3$, and ϵ_4.

Among the singular surfaces of a CMG system, of a special interest is the angular momentum envelope that is defined as the boundary of the maximum workspace of the total angular momentum $\boldsymbol{H}$. The angular momentum envelope of a CMG cluster in a pyramid configuration consists of two types of singular surfaces which are connected to each other smoothly. The first type corresponds to the case when all ϵ_i are positive, that is, the angular momentum of each CMG unit has a maximal projection onto the singular direction, as shown in Fig. 4a. (The case of all negative ϵ_i is also on the angular momentum envelope due to symmetry.) Notice that this singular surface does not cover the whole momentum envelope, and there exist holes on the surface. These holes are smoothly connected to the second type of singular surface, for which one and only one of the ϵ_i, $i \in \{1, \ldots, N\}$, is negative (or only one positive due to symmetry).[1,4] This singular surface produces a trumpetlike funnel at the holes, which completes the envelope and is shown in Fig. 4b.

In conclusion, the complete momentum envelope is composed of the singular surface with $\epsilon_i > 0$ for $i = 1, \ldots, N$ and the external portion of the singular surface with one and only one negative ϵ_i. Figure 5 shows the complete angular momentum envelop with a cut revealing part of the rather complicated internal singular surface.

IV. Singularity Analysis of VSCMGs Without Power Tracking

Whereas the gimbal rates $\dot{\gamma}_i$ are the only control input variables in a CMG system, the wheel accelerations $\dot{\Omega}_i$ offer additional control

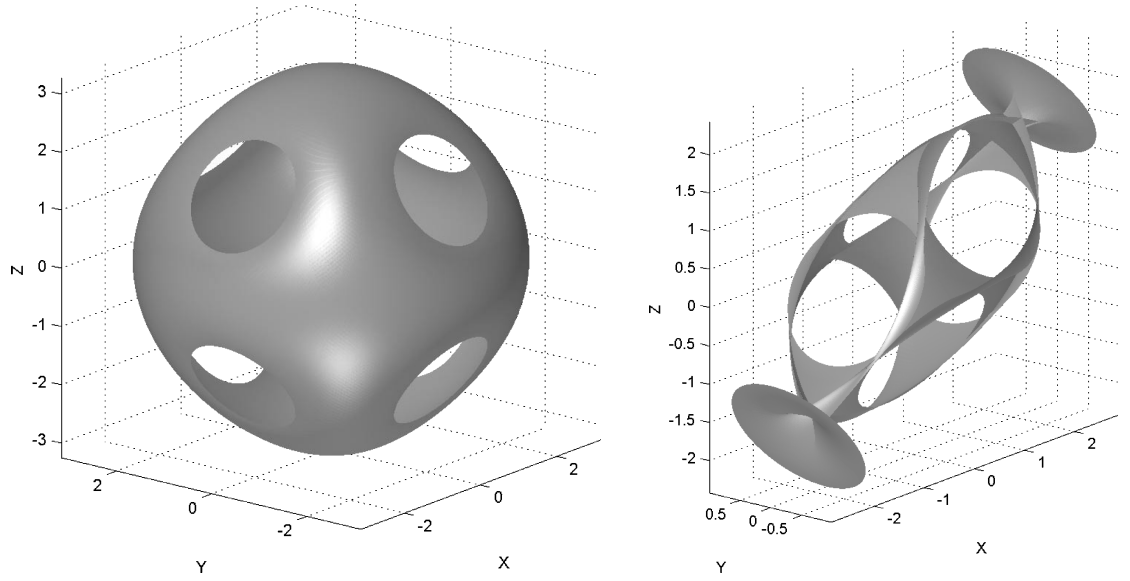

a) $\epsilon_1 = \epsilon_2 = \epsilon_3 = \epsilon_4 = +1$ **b)** $\epsilon_1 = -1, \epsilon_2 = \epsilon_3 = \epsilon_4 = +1$

Fig. 4 Singular surfaces of CMGs in pyramid configuration.

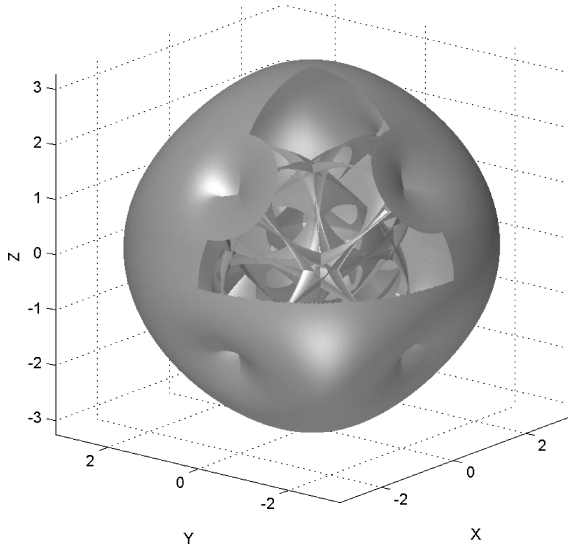

Fig. 5 Angular momentum envelope of CMGs.

variables in the case of a VSCMG system. The torque equation (7) for a CMG cluster has to be modified in the case of VSCMGs as

$$[C(\boldsymbol{\Omega}, \gamma) \quad D(\gamma)] \begin{bmatrix} \dot{\gamma} \\ \dot{\boldsymbol{\Omega}} \end{bmatrix} = \boldsymbol{T}$$

When rank $C(\boldsymbol{\Omega}, \gamma) = 2$, there exists a singular direction $\boldsymbol{u}$ perpendicular to this plane, that is, $\boldsymbol{u}^T \boldsymbol{t}_i = 0$ for all $i = 1, \ldots, N$, and the condition for singularity, therefore, remains the same as for the CMG case; see Eqs. (8).

Schaub et al.[13] introduced a technique to cope with this type of singularity of the matrix C using the weighted minimum norm solution of Eq. (4), namely,

$$\begin{bmatrix} \dot{\gamma} \\ \dot{\boldsymbol{\Omega}} \end{bmatrix} = W Q^T (Q W Q^T)^{-1} \boldsymbol{T} \tag{13}$$

where $Q \triangleq [C \;\; D]$ and W is a weighting matrix, which is function of the singularity index of the matrix C,[13,15] for instance,

$$W \triangleq \begin{bmatrix} w_1 e^{-w_2 \kappa(C)} \boldsymbol{I}_N & 0_N \\ 0_N & \boldsymbol{I}_N \end{bmatrix} \tag{14}$$

where $\kappa(C)$ is the condition number of the matrix C and w_1 and w_2 are positive constants. According to this approach, the VSCMGs operate as CMGs to take full advantage of the torque amplification effect under normal conditions, that is, $\kappa(C)$ is small, but as the singularity is approached, $\kappa(C)$ becomes large and the VSCMGs smoothly switch to a momentum wheel mode.[13,15] However, this technique is a passive method that by itself does not ensure avoidance of singularities. Therefore, an active method to avoid the singularity is needed.

For this purpose, let us consider the possibility of null motion for a VSCMG system. Such a null motion must satisfy

$$[C \;\; D] \begin{bmatrix} \dot{\gamma} \\ \dot{\boldsymbol{\Omega}} \end{bmatrix}_{\text{null}} = \boldsymbol{0}_{3\times 1} \tag{15}$$

Equivalently, a null motion strategy will not change the total angular momentum $\boldsymbol{H}$. Notice that $\dot{\gamma} \in \mathcal{N}(C)$ and $\dot{\boldsymbol{\Omega}} \in \mathcal{N}(D)$ is a sufficient but not necessary condition for the existence of null motion. Even if $\dot{\gamma} \notin \mathcal{N}(C)$ and $\dot{\boldsymbol{\Omega}} \notin \mathcal{N}(D)$, there still exists the possibility of satisfying Eq. (15). In fact, there always exists a null motion solution $[\dot{\gamma}^T \; \dot{\boldsymbol{\Omega}}^T]^T_{\text{null}}$ satisfying Eq. (15), if $N > 2$.

Our objective is to investigate the possibility of escaping from a singularity using null motion. Mathematically, we are interested in conditions such that the following is true: at time t,

$$C[\boldsymbol{\Omega}(t), \gamma(t)]\dot{\gamma}(t) + D[\gamma(t)]\dot{\boldsymbol{\Omega}}(t) = 0 \tag{16}$$

and at time $t + \mathrm{d}t$,

$$C[\boldsymbol{\Omega}(t + \mathrm{d}t), \gamma(t + \mathrm{d}t)]\dot{\gamma}(t + \mathrm{d}t) + D[\gamma(t + \mathrm{d}t)]\dot{\boldsymbol{\Omega}}(t + \mathrm{d}t) = 0 \tag{17}$$

where $C(\boldsymbol{\Omega}, \gamma)$ and $D(\gamma)$ as in Eqs. (5) and (6). Using Taylor's theorem, one obtains

$$\gamma(t + \mathrm{d}t) = \gamma(t) + \dot{\gamma}(t)\mathrm{d}t + r_1(\mathrm{d}t)$$

$$\dot{\gamma}(t + \mathrm{d}t) = \dot{\gamma}(t) + \ddot{\gamma}(t)\mathrm{d}t + r_2(\mathrm{d}t)$$

$$\boldsymbol{\Omega}(t + \mathrm{d}t) = \boldsymbol{\Omega}(t) + \dot{\boldsymbol{\Omega}}(t)\mathrm{d}t + r_3(\mathrm{d}t)$$

$$\dot{\boldsymbol{\Omega}}(t + \mathrm{d}t) = \dot{\boldsymbol{\Omega}}(t) + \ddot{\boldsymbol{\Omega}}(t)\mathrm{d}t + r_4(\mathrm{d}t)$$

where $\lim_{\mathrm{d}t \to 0} \|r_i(\mathrm{d}t)\|/\mathrm{d}t = 0, i = 1, \ldots, 4$. The question of existence of null motion, therefore, reduces to one of finding

$[\ddot{\gamma}^T(t)\ddot{\Omega}^T(t)]^T \in \mathbb{R}^{2N}$ such that Eq. (17) holds, given that Eq. (16) holds. Noticing that

$$C[\Omega(t+\mathrm{d}t), \gamma(t+\mathrm{d}t)] = C[\Omega(t), \gamma(t)] + \sum_{i=1}^{N} \frac{\partial C}{\partial \gamma_i}\dot{\gamma}_i(t)\mathrm{d}t + \sum_{i=1}^{N} \frac{\partial C}{\partial \Omega_i}\dot{\Omega}_i(t)\mathrm{d}t + r_5(\mathrm{d}t)$$

$$D[\gamma(t+\mathrm{d}t)] = D[\gamma(t)] + \sum_{i=1}^{N} \frac{\partial D}{\partial \gamma_i}\dot{\gamma}_i(t)\mathrm{d}t + r_6(\mathrm{d}t)$$

where $\lim_{\mathrm{d}t\to 0} \|r_i(\mathrm{d}t)\|/\mathrm{d}t = 0$, $i = 5, 6$, we have from Eq. (17) that

$$0 = C[\Omega(t), \gamma(t)]\ddot{\gamma}(t) + D[\gamma(t)]\ddot{\Omega}(t) + \left[\sum_{i=1}^{N} \frac{\partial C}{\partial \gamma_i}\dot{\gamma}_i(t)\mathrm{d}t\right]\dot{\gamma}(t) + \left[\sum_{i=1}^{N} \frac{\partial C}{\partial \Omega_i}\dot{\Omega}_i(t)\mathrm{d}t\right]\dot{\gamma}(t) + C[\Omega(t), \gamma(t)]\ddot{\gamma}(t)\mathrm{d}t + \left[\sum_{i=1}^{N} \frac{\partial D}{\partial \gamma_i}\dot{\gamma}_i(t)\mathrm{d}t\right]\dot{\Omega}(t) + D[\gamma(t)]\ddot{\Omega}(t)\mathrm{d}t + r_7(\mathrm{d}t) \quad (18)$$

with $\lim_{\mathrm{d}t\to 0} \|r_7(\mathrm{d}t)\|/\mathrm{d}t = 0$. Using Eq. (16), dividing with $\mathrm{d}t$, and taking the limit as $\mathrm{d}t \to 0$, we have that a null motion exists if and only if there exist $\ddot{\gamma}(t) \in \mathbb{R}^N$ and $\ddot{\Omega}(t) \in \mathbb{R}^N$ such that the following is true:

$$0 = C(\Omega(t), \gamma(t))\ddot{\gamma}(t) + D(\gamma(t))\ddot{\Omega}(t) + \left[\sum_{i=1}^{N} \frac{\partial C}{\partial \gamma_i}\dot{\gamma}_i(t)\right]\dot{\gamma}(t) + \left[\sum_{i=1}^{N} \frac{\partial C}{\partial \Omega_i}\dot{\Omega}_i(t)\right]\dot{\gamma}(t) + \left[\sum_{i=1}^{N} \frac{\partial D}{\partial \gamma_i}\dot{\gamma}_i(t)\right]\dot{\Omega}(t) \quad (19)$$

Condition (19) can be written as

$$\left[C[\Omega(t), \gamma(t)]\, D[\gamma(t)]\right]\begin{bmatrix}\ddot{\gamma}(t)\\ \ddot{\Omega}(t)\end{bmatrix} = -2\sum_{i=1}^{N} I_{\mathrm{ws}i}\boldsymbol{t}_i\dot{\gamma}_i\dot{\Omega}_i + \sum_{i=1}^{N} I_{\mathrm{ws}i}\Omega_i\boldsymbol{s}_i\dot{\gamma}_i^2 \quad (20)$$

where $[\dot{\gamma}^T(t), \dot{\Omega}^T(t)]^T \in \mathcal{N}([C\ D])$. Because the column vectors of $[C\ D]$ always span the three-dimensional space, there always exist vectors $\ddot{\gamma}(t) \in \mathbb{R}^N$ and $\ddot{\Omega}(t) \in \mathbb{R}^N$ that satisfy Eq. (20). Thus, a null motion always exists for the VSCMG case. Most interestingly, we do not need all N wheels to operate as VSCMGs to avoid singularities. Only two out of all N wheels need to operate as VSCMGs, whereas the remaining $N-2$ may operate as conventional CMGs. This is because any two inner products $\boldsymbol{u}\cdot\boldsymbol{s}_i$ cannot be zero at a singularity simultaneously, provided that no two gimbal directions are identical. We conclude that every singularity (in terms of the rank deficiency of C) is escapable with null motion $[\dot{\gamma}^T, \dot{\Omega}^T]^T_{\mathrm{null}} \in \mathcal{N}([C\ D])$, if we have no less than two VSCMGs out of a total of N wheels.

Remark: The preceding analysis can be easily adapted to investigate the existence of null motions for a conventional CMGs cluster. By setting $h_i = 1$ for all $i = 1, \ldots, N$ and $\dot{\Omega}(t) \equiv \ddot{\Omega}(t) \equiv \mathbf{0}_{N\times 1}$ in Eq. (19), one obtains the following condition for existence of null motion for the CMG case as

$$C[\gamma(t)]\,\ddot{\gamma}(t) = D[\gamma(t)]\dot{\gamma}^2(t) \quad (21)$$

where $\dot{\gamma}^2 \triangleq [\dot{\gamma}_1^2, \ldots, \dot{\gamma}_N^2]^T$ and $C[\gamma(t)]\dot{\gamma}(t) = 0$. There exists $\dot{\gamma}(t) \in \mathcal{N}[C(\gamma(t))]$ such that Eq. (21) has a solution for some $\ddot{\gamma}(t) \in \mathbb{R}^N$ if and only if there exists $\dot{\gamma}(t) \in \mathcal{N}[C(\gamma(t))]$ such that $D[\gamma(t)]\dot{\gamma}^2(t) \in \mathcal{R}[C(\gamma(t))]$, equivalently, $\boldsymbol{v}^T D[\gamma(t)]\dot{\gamma}^2(t) = 0$, for all nonzero $\boldsymbol{v} \in \mathcal{R}^{\perp}[C(\gamma(t))]$. Now recall that $\mathcal{R}^{\perp}[C(\gamma(t))] = \mathrm{span}\{\boldsymbol{u}\}$; hence, the condition for existence of a solution to condition (21) is that

$$\exists \dot{\gamma} \in \mathcal{N}[C(\gamma_s)] \quad \text{such that} \quad \boldsymbol{u}^T D(\gamma_s)\dot{\gamma}^2 = 0 \quad (22)$$

Notice now that $\boldsymbol{u}^T D(\gamma_s)\dot{\gamma}^2 = \dot{\gamma}^T\mathcal{P}\dot{\gamma}$, where $\mathcal{P} \triangleq \mathrm{diag}[\boldsymbol{u}^T\boldsymbol{s}_1, \ldots, \boldsymbol{u}^T\boldsymbol{s}_N]$. Therefore, condition (22) takes the form

$$\exists \dot{\gamma} \in \mathcal{N}[C(\gamma(t))] \quad \text{such that} \quad \dot{\gamma}^T\mathcal{P}\dot{\gamma} = 0 \quad (23)$$

Condition (23) for the existence of null motion is identical to the condition obtained in Ref. 21. However, the preceding method is more straightforward and avoids using the concept of virtual gimbal angle displacements, which is to some degree, a mathematical artifact; also see Ref. 19.

V. Singularity Avoidance Using Null Motion of VSCMGs Without Power Tracking

Let $\kappa(\gamma, \Omega)$ be a measure of the singularity of the matrix $C(\Omega, \gamma)$ that is a function of the gimbal angles and wheel speeds. Without loss of generality, let $\kappa(\gamma, \Omega)$ be the condition number of the matrix C. [Among the several choices of $\kappa(\gamma, \Omega)$, the condition number has been selected as a measure of the singularity in this paper because it is known that it is a more reliable measure of rank deficiency of a matrix than, for example, the determinant of the matrix.[23]] The condition number of C has to be kept small to avoid any singularities. The proposed method, commonly, known as the gradient method,[4] adds a null motion that does not have any effect on the generated output torque but it decreases the singularity measure $\kappa(\gamma, \Omega)$. For example, if we let $Q = [C\ D]$, then any null motion can be written as

$$\begin{bmatrix}\dot{\gamma}\\ \dot{\Omega}\end{bmatrix}_{\mathrm{null}} = [\boldsymbol{I}_{2N} - \tilde{W}Q^T(Q\tilde{W}Q^T)^{-1}Q]\tilde{W}\,\boldsymbol{d}, \qquad \boldsymbol{d} \in \mathbb{R}^{2N\times 1} \quad (24)$$

where $\tilde{W} > 0$ is some weighting matrix that can be used to distribute the control input between gimbal rate and wheel speed acceleration. It can be easily shown that $Q[\dot{\gamma}^T, \dot{\Omega}^T]^T_{\mathrm{null}} = 0$ and that the matrix $[\boldsymbol{I}_{2N} - \tilde{W}Q^T(Q\tilde{W}Q^T)^{-1}Q]\tilde{W}$ is positive semidefinite. If the vector $\boldsymbol{d}$ is selected as

$$\boldsymbol{d} = -k\begin{bmatrix}\dfrac{\partial\kappa}{\partial\gamma}^T\\ \dfrac{\partial\kappa}{\partial\Omega}^T\end{bmatrix}, \qquad k > 0 \quad (25)$$

then, the rate of change of $\kappa(\gamma, \Omega)$ due to Eq. (24) is

$$\dot{\kappa}_{\mathrm{null}} = \begin{bmatrix}\dfrac{\partial\kappa}{\partial\gamma} & \dfrac{\partial\kappa}{\partial\Omega}\end{bmatrix}\begin{bmatrix}\dot{\gamma}\\ \dot{\Omega}\end{bmatrix}_{\mathrm{null}} = -k\begin{bmatrix}\dfrac{\partial\kappa}{\partial\gamma} & \dfrac{\partial\kappa}{\partial\Omega}\end{bmatrix} \times [\boldsymbol{I}_{2N} - \tilde{W}Q^T(Q\tilde{W}Q^T)^{-1}Q]\tilde{W}\begin{bmatrix}\dfrac{\partial\kappa}{\partial\gamma}^T\\ \dfrac{\partial\kappa}{\partial\Omega}^T\end{bmatrix} \le 0 \quad (26)$$

Therefore, it is expected that the singularity will be avoided. However, this method does not necessarily guarantee singularity avoidance, because the change of $\kappa(\gamma, \Omega)$ due to the torque-generating solution of Eq. (13) may dominate the change due to the null motion of Eq. (24). Nevertheless, singularity avoidance methods based on null motions have been successfully used in practice.[4,20] If a condition number is chosen for κ, Schaub and Junkins[20] provide an algorithm to quickly compute $\partial\kappa/\partial\gamma$. The other sensitivity $\partial\kappa/\partial\Omega$ also can be computed in similar way; also see Ref. 24. Finally, we point out that, although Eq. (24) looks similar to Eq. (16) of Ref. 20, the latter is missing the postmultiplication by the matrix $\tilde{W}$. Without it one cannot ensure that $\dot{\kappa}_{\mathrm{null}} \le 0$.

VI. Singularity Analysis of VSCMGs with Power Tracking

In Ref. 14, the authors have introduced a control method for the simultaneous attitude and power tracking problem for the case of a rigid spacecraft with N momentum wheels. These results have been extended to the case of N VSCMGs in Refs. 15 and 18. By setting the gimbal angles in Ref. 15 to be constant, one can retrieve the results of Ref. 14 as a special case.

The total kinetic energy stored in the wheels of the VSCMG cluster is

$$E \triangleq \tfrac{1}{2}\boldsymbol{\Omega}^T I_{\mathrm{ws}}\boldsymbol{\Omega} \tag{27}$$

where $I_{\mathrm{ws}} \triangleq \mathrm{diag}[I_{\mathrm{ws}_1}, \ldots, I_{\mathrm{ws}_N}] \in \mathbb{R}^{N\times N}$. Hence, the power (rate of change of the energy) is given by

$$P = \frac{\mathrm{d}E}{\mathrm{d}t} = \boldsymbol{\Omega}^T I_{\mathrm{ws}}\dot{\boldsymbol{\Omega}} = \begin{bmatrix}0 & \boldsymbol{\Omega}^T I_{\mathrm{ws}}\end{bmatrix}\begin{bmatrix}\dot{\boldsymbol{\gamma}}\\ \dot{\boldsymbol{\Omega}}\end{bmatrix} \tag{28}$$

This equation is augmented to the attitude tracking equation (4), to obtain

$$Q_p\boldsymbol{u} = \boldsymbol{L} \tag{29}$$

where

$$\boldsymbol{u} \triangleq \begin{bmatrix}\dot{\boldsymbol{\gamma}}\\ \dot{\boldsymbol{\Omega}}\end{bmatrix}, \qquad Q_p \triangleq \begin{bmatrix}C(\boldsymbol{\Omega},\boldsymbol{\gamma}) & D(\boldsymbol{\gamma})\\ \mathbf{0}_{1\times N} & \boldsymbol{\Omega}^T I_{\mathrm{ws}}\end{bmatrix}, \qquad \boldsymbol{L} \triangleq \begin{bmatrix}\boldsymbol{T}\\ P\end{bmatrix}$$

The existence of a solution to Eq. (29) depends on the rank of the coefficient matrix $Q_p \in \mathbb{R}^{4\times 2N}$. If rank $Q_p = 4$, then Eq. (29) always has a solution, for example,

$$\begin{bmatrix}\dot{\boldsymbol{\gamma}}\\ \dot{\boldsymbol{\Omega}}\end{bmatrix} = W Q_p^T\left(Q_p W Q_p^T\right)^{-1}\boldsymbol{L} \tag{30}$$

for some $2N\times 2N$ weighting matrix W. However, if rank $Q_p = 3$, it is not possible to solve Eq. (29). (Notice that rank $Q_p \geq 3$, because rank $[C(\boldsymbol{\Omega},\boldsymbol{\gamma})\ D(\boldsymbol{\gamma})] = 3$ for all $\boldsymbol{\Omega}\in\mathbb{R}^N$ and $\boldsymbol{\gamma}\in[0, 2\pi)^N$.) In Ref. 15, the authors have shown that a sufficient (but not necessary) condition for rank $Q_p = 4$ is that rank $C = 3$. This means that the issue of singularity avoidance for a VSCMGs system (in terms of the rank deficiency of C) becomes more pronounced in case of a power tracking requirement.

To investigate the existence of null motion for the case of both attitude and power tracking problem, we first notice that in this case, in addition to conditions (16) and (17), the following conditions must be true as well: at time t,

$$\boldsymbol{\Omega}^T(t) I_{\mathrm{ws}}\dot{\boldsymbol{\Omega}}(t) = 0 \tag{31}$$

and at time $t + \mathrm{d}t$,

$$\boldsymbol{\Omega}^T(t+\mathrm{d}t) I_{\mathrm{ws}}\dot{\boldsymbol{\Omega}}(t+\mathrm{d}t) = 0 \tag{32}$$

leading to the condition that a null motion exists if and only if there exist $\ddot{\boldsymbol{\gamma}}(t) \in \mathbb{R}^N$ and $\dot{\boldsymbol{\Omega}}(t) \in \mathbb{R}^N$ such that

$$\begin{bmatrix}C[\boldsymbol{\Omega}(t),\boldsymbol{\gamma}(t)] & D[\boldsymbol{\gamma}(t)]\\ \mathbf{0}_{1\times N} & \boldsymbol{\Omega}^T(t) I_{\mathrm{ws}}\end{bmatrix}\begin{bmatrix}\ddot{\boldsymbol{\gamma}}(t)\\ \dot{\boldsymbol{\Omega}}(t)\end{bmatrix} = \begin{bmatrix}\boldsymbol{\zeta}_1\\ \zeta_2\end{bmatrix} \tag{33}$$

where $\boldsymbol{\zeta}_1 \in \mathbb{R}^3$ and $\zeta \in \mathbb{R}$ from

$$\boldsymbol{\zeta}_1 \triangleq -2\sum_{i=1}^{N} I_{\mathrm{ws}i}\boldsymbol{t}_i\dot{\gamma}_i\dot{\Omega}_i + \sum_{i=1}^{N} I_{\mathrm{ws}i}\Omega_i\boldsymbol{s}_i\dot{\gamma}_i^2 \tag{34}$$

$$\zeta_2 \triangleq -\dot{\boldsymbol{\Omega}}^T I_{\mathrm{ws}}\dot{\boldsymbol{\Omega}} = -\sum_{i=1}^{N} I_{\mathrm{ws}_i}\dot{\Omega}_i^2 \tag{35}$$

Next, we show that a solution to Eq. (33) exists if and only if rank $M = 2$, where

$$M \triangleq \begin{bmatrix}I_{\mathrm{ws}_1}\boldsymbol{u}^T\boldsymbol{s}_1 & I_{\mathrm{ws}_2}\boldsymbol{u}^T\boldsymbol{s}_2 & \cdots & I_{\mathrm{ws}_N}\boldsymbol{u}^T\boldsymbol{s}_N\\ I_{\mathrm{ws}_1}\Omega_1 & I_{\mathrm{ws}_2}\Omega_2 & \cdots & I_{\mathrm{ws}_N}\Omega_N\end{bmatrix} \tag{36}$$

To this end, notice that a solution to Eq. (33) exists if and only if $\boldsymbol{\zeta} \triangleq [\boldsymbol{\zeta}_1^T\ \zeta_2]^T \in \mathcal{R}[Q_p]$, equivalently, if and only if $\boldsymbol{v}^T\boldsymbol{\zeta} = 0$ for all nonzero $\boldsymbol{v} \in \mathcal{R}^{\perp}[Q_p]$. Notice that

$$\mathcal{R}^{\perp}[Q_p] = \{\boldsymbol{v} = \begin{bmatrix}\boldsymbol{v}_1^T & v_2\end{bmatrix}^T \in \mathbb{R}^4 : \boldsymbol{v}_1 \in \mathcal{R}^{\perp}(C),\ \boldsymbol{v}_1^T D(\boldsymbol{\gamma}) + v_2\boldsymbol{\Omega}^T I_{\mathrm{ws}} = 0\} \tag{37}$$

which, via the fact that $\mathcal{R}^{\perp}(C) = \mathrm{span}\{\boldsymbol{u}\}$, leads to the condition

$$[\boldsymbol{u}^T\ \eta]\begin{bmatrix}\boldsymbol{\zeta}_1\\ \zeta_2\end{bmatrix} = \sum_{i=1}^{N} I_{\mathrm{ws}i}\boldsymbol{u}^T\boldsymbol{s}_i\Omega_i\dot{\gamma}_i^2 - \eta\left(\sum_{i=1}^{N} I_{\mathrm{ws}_i}\dot{\Omega}_i^2\right) = 0 \tag{38}$$

for all η such that $\boldsymbol{u}^T D(\boldsymbol{\gamma}) + \eta\,\boldsymbol{\Omega}^T I_{\mathrm{ws}} = 0$, that is, for all η such that

$$\left[I_{\mathrm{ws}_1}\boldsymbol{u}^T\boldsymbol{s}_1, \ldots, I_{\mathrm{ws}_N}\boldsymbol{u}^T\boldsymbol{s}_N\right] + \eta\left[I_{\mathrm{ws}_1}\Omega_1, \ldots, I_{\mathrm{ws}_N}\Omega_N\right] = 0 \tag{39}$$

If rank $M = 2$, then there does not exist an $\eta \in \mathbb{R}$ that satisfies Eq. (39), thus, sufficiency follows. On the other hand, if rank $M = 1$, then there exists a nonzero scalar η satisfying Eq. (39). This yields

$$I_{\mathrm{ws}_i}\boldsymbol{u}^T\boldsymbol{s}_i = -\eta I_{\mathrm{ws}_i}\Omega_i, \qquad i = 1, \ldots, N$$

Thus, Eq. (38) becomes

$$-\eta\left(\sum_{i=1}^{N} I_{\mathrm{ws}i}\Omega_i^2\dot{\gamma}_i^2 + \sum_{i=1}^{N} I_{\mathrm{ws}_i}\dot{\Omega}_i^2\right) = 0 \tag{40}$$

which cannot hold for any $[\dot{\boldsymbol{\gamma}}, \dot{\boldsymbol{\Omega}}] \neq 0$.

In case rank $M = 1$, it is, therefore, impossible to satisfy both the angular momentum (torque) and the kinetic energy (power) requirements for singularity avoidance using null motion. Therefore, the inescapable singularities of a VSCMG system used for combined attitude control and power tracking is completely characterized by the rank of the matrix M in Eq. (36). Notice that because the wheel speeds Ω_i are all positive by the definition of the spin axes $\boldsymbol{s}_i$, the rank deficiency of M can occur only when $\epsilon_i \triangleq \mathrm{sign}(\boldsymbol{u}\cdot\boldsymbol{s}_i) = +1$ for all $i = 1, \ldots, N$.

VII. Angular Momentum Envelopes of a VSCMG Cluster

In this section, the inescapable singularities of a VSCMG system and their relation to the rank deficiency of the matrix M in Eq. (36) are studied in more detail. For this purpose, we introduce three singular surfaces in the three-dimensional angular momentum space. The first surface is the momentum envelope for given kinetic energy, the second surface is the momentum envelope for given wheel speeds, and the third surface is the momentum envelope for given kinetic energy and gimbal angles. With the help of these three surfaces, we can visualize the geometric conditions under which a singularity is either escapable or inescapable.

A. Momentum Envelope for Given Kinetic Energy

In this section, we define the angular momentum envelope of a VSCMG cluster for a given kinetic energy, and we show that the total angular momentum vector reaches this envelope if and only if the VSCMG cluster encounters an inescapable singularity, that is, rank $M = 1$.

To this end, consider the case when a power command $P(t)$ is given for all $t_0 \le t \le t_f$. Then the kinetic energy stored in the VSCMG cluster for $t \ge t_0$ can be computed from

$$E(t) = \int_{t_0}^{t} P(t)\,\mathrm{d}t + E(t_0)$$

Suppose that $E(\bar{t})$ is given at some instant $t = \bar{t}$. The objective is to find the maximum workspace of $\boldsymbol{H}(\bar{t})$ with the given value of the kinetic energy. The boundary of the maximum angular momentum workspace can be found by solving the following maximization problem.

For a given singular direction $\boldsymbol{u}$, find the gimbal angles γ_i and wheel speeds Ω_i that maximize the function $\mathcal{J}$ defined by

$$\mathcal{J} \triangleq \boldsymbol{H}\cdot\boldsymbol{u} = \sum_{i=1}^{N} I_{\mathrm{ws}_i}\Omega_i \boldsymbol{u}\cdot\boldsymbol{s}_i = \sum_{i=1}^{N} \alpha_i(\gamma_i) I_{\mathrm{ws}_i}\Omega_i \tag{41}$$

subject to the constraints

$$\sum_{i=1}^{N} I_{\mathrm{ws}_i}\Omega_i^2 = 2E \tag{42}$$

$$\alpha_i^2(\gamma_i) \le \alpha_{\max_i}^2, \qquad i = 1, \ldots, N \tag{43}$$

where $\alpha_i(\gamma_i) \triangleq \boldsymbol{u}\cdot\boldsymbol{s}_i$ and $\alpha_{\max_i}$ is its maximum value. Because α_i becomes maximum when $\boldsymbol{s}_i$ has a maximum projection onto $\boldsymbol{u}$ as shown in Fig. 3, $\alpha_{\max_i}$ is given by $\alpha_{\max_i} = \sqrt{[1-(\boldsymbol{g}_i\cdot\boldsymbol{u})^2]}$.

In Appendix A, it is shown that the solution to this maximization problem is

$$\alpha_i^* = \alpha_{\max_i}, \qquad \Omega_i^* = \frac{\alpha_{\max_i}}{2\lambda_0^*}, \qquad i = 1, \ldots, N \tag{44}$$

where

$$\lambda_0^* \triangleq \frac{1}{\sqrt{8E}}\left(\sum_{i=1}^{N} I_{\mathrm{ws}_i}\alpha_{\max_i}^2\right)^{\frac{1}{2}}$$

Equation (44) implies that the gimbal angles of the VSCMGs are in a singular configuration with all $\epsilon_i = +1$ and that each wheel has a speed that is proportional to $\boldsymbol{u}\cdot\boldsymbol{s}_i$. It can also be shown that the solution (44) corresponds to an inescapable singularity when rank $M = 1$. (See Appendix A for the details.) In summary, an inescapable singularity for the case of attitude/power tracking for a VSCMG cluster occurs when the wheels have maximum angular momentum along the singular direction with the given kinetic energy constraint.

The preceding observations also lend themselves to a method for drawing the angular momentum envelope of a VSCMGs system with given kinetic energy constraint. Given a singular direction $\boldsymbol{u}$, each spin axis $\boldsymbol{s}_i$ is determined as in the conventional CMGs case, that is, from Eq. (11) with all $\epsilon_i = +1$ and with the wheel speeds determined from Eq. (44). Hence, the total angular momentum at this singular configuration for a given singular direction $\boldsymbol{u}$ can be expressed as

$$\boldsymbol{H} = \sum_{i=1}^{N} \frac{(\boldsymbol{g}_i\times\boldsymbol{u})\times\boldsymbol{g}_i}{|\boldsymbol{g}_i\times\boldsymbol{u}|}\Omega_i^* I_{\mathrm{ws}_i} = \frac{1}{2\lambda_0^*}\sum_{i=1}^{N}[\boldsymbol{u}-\boldsymbol{g}_i(\boldsymbol{g}_i\cdot\boldsymbol{u})]I_{\mathrm{ws}_i} \tag{45}$$

where the last equality follows from $|\boldsymbol{g}_i\times\boldsymbol{u}| = \max\{\boldsymbol{s}_i\cdot\boldsymbol{u}\} = \alpha_{\max_i}$.

Equation (45) defines an ellipsoid in the momentum space. If the total angular momentum vector reaches this surface and the reference attitude (torque requirement) forces it to go outside this surface, then the VSCMGs cluster cannot meet both attitude and power tracking requirements. Contrary to the CMGs case, shown in Fig. 4a, the momentum envelope of a VSCMG cluster with given kinetic energy has no holes. The reason is that, when the singular direction $\boldsymbol{u}$ is along a gimbal axis $\boldsymbol{g}_i$, the angular speed of the ith wheel does not have a component along $\boldsymbol{u}$ because $\boldsymbol{s}_i \perp \boldsymbol{g}_i$ and, thus, $\boldsymbol{s}_i \perp \boldsymbol{u}$. Hence, the ith wheel speed does not contribute to the maximization of the total angular momentum along $\boldsymbol{u}$. Thus, Ω_i may be taken to be zero with all of the other wheels having higher speeds (to satisfy the kinetic energy constraint).

B. Geometric Picture of the Inescapable Singularity Case

A nice geometric picture emerges for describing the occurrence of inescapable singularities using the earlier concept of the angular momentum envelope. In addition to the angular momentum envelope for given kinetic energy introduced in the preceding section, one can also define the angular momentum envelope of a VSCMG system with given energy and a given set of gimbal angles. Given the total kinetic energy E and the gimbal angles, this envelope is defined as the boundary of the maximum workspace of the total momentum $\boldsymbol{H}$ as the wheel speeds vary but the total energy E and the gimbal angles γ_i are kept constant. This surface can be drawn by solving the following maximization problem.

Maximize

$$\mathcal{J} \triangleq \boldsymbol{H}\cdot\boldsymbol{u} = \sum_{i=1}^{N} I_{\mathrm{ws}_i}\Omega_i \boldsymbol{u}\cdot\boldsymbol{s}_i = \sum_{i=1}^{N} \alpha_i I_{\mathrm{ws}_i}\Omega_i \tag{46}$$

subject to the constraint

$$\sum_{i=1}^{N} I_{\mathrm{ws}_i}\Omega_i^2 = 2E$$

for each $\boldsymbol{u}\in\mathbb{R}^3$, $\|\boldsymbol{u}\| = 1$, while the gimbal angles γ_i are fixed.

The procedure for solving this maximization problem is similar to the one in Sec. VII.A, and thus, it is omitted. Its solution yields

$$\Omega_i^* = \alpha_i \big/ 2\lambda_0^*$$

where

$$\lambda_0^* \triangleq \frac{1}{\sqrt{8E}}\left(\sum_{i=1}^{N} I_{\mathrm{ws}_i}\alpha_i^2\right)^{\frac{1}{2}}$$

In addition to the angular momentum envelope for given kinetic energy, and the envelope with given kinetic energy and gimbal angles, one can also construct the angular momentum envelope for given wheel speeds using the method described in Sec. III.A. The interplay between the latter two surfaces provides a clear picture for the occurrence of the inescapable singularities.

Figures 6 and 7 show these three envelopes at a singular configuration corresponding to the singular direction $\boldsymbol{u} = [0, 0, 1]^T$ with $\epsilon_i > 0$ for $i = 1, 2, 3$, and 4. In Figs. 6 and 7, surface A is the momentum envelope with given wheel speeds, surface B is the momentum envelope with given energy and gimbal angles, and surface C is the momentum envelope with given kinetic energy.

Figure 6 shows a case when the gimbal angles are singulary configured with all $\epsilon_i > 0$, but the wheel speeds are not equal to the maximizing solution of Eq. (44), hence, rank $M \ne 1$. Notice that the total momentum vector $\boldsymbol{H}$ lies inside the momentum envelope with given energy (surface C). As the gimbal angles vary with the wheel speeds fixed, $\boldsymbol{H}$ will move inside the surface A; thus, the projection of the change of the angular momentum due to the gimbal changes along the singular direction is $\Delta\boldsymbol{H}\cdot\boldsymbol{u}|_{\dot{\gamma}} < 0$. As the wheel speeds vary with gimbal angles and total energy fixed, $\boldsymbol{H}$ will move inside the surface B; thus, the projection of the change of the angular momentum due to the wheel speed changes along the singular direction, $\Delta\boldsymbol{H}\cdot\boldsymbol{u}|_{\dot{\Omega}}$, can be either positive or negative. This is shown in Fig. 6. Hence, the term $\Delta\boldsymbol{H}\cdot\boldsymbol{u}|_{\dot{\Omega}}$ can cancel the negative term $\Delta\boldsymbol{H}\cdot\boldsymbol{u}|_{\dot{\gamma}}$. Therefore, a gimbal angle change is possible without violating the angular momentum and energy constraints. As a result, in this case the singularity is escapable using null motion. On the other hand, Fig. 7 shows an inescapable singularity, that is, when rank $M = 1$. The momentum vector $\boldsymbol{H}$ reaches the envelope C. At this value of $\boldsymbol{H}$,

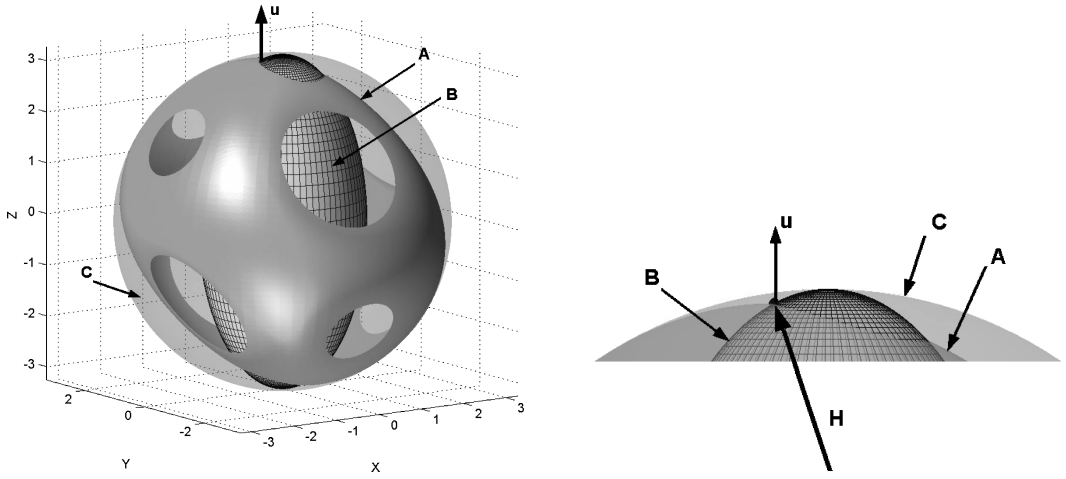

Fig. 6 Escapable singularity of VSCMG.

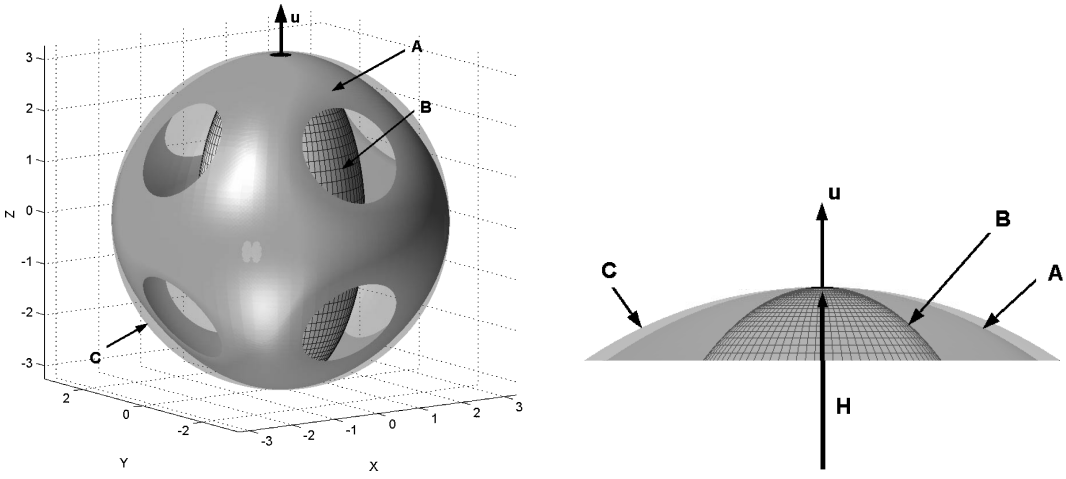

Fig. 7 Inescapable singularity of VSCMG.

both surface A and surface B are normal to the singular direction $\boldsymbol{u}$, and so both $\Delta \boldsymbol{H}\cdot\boldsymbol{u}|_{\dot{\gamma}}$ and $\Delta \boldsymbol{H}\cdot\boldsymbol{u}|_{\Omega}$ are negative. Therefore, these two cannot cancel each other. This means that gimbal angle changes and wheel speed changes while $\Delta \boldsymbol{H}=0$ is impossible. Thus, escaping from the singularity without violating either the momentum or the power constraints is impossible.

VIII. Condition for Singularity Avoidance

If a VSCMGs cluster has a pyramid configuration with skew angle θ (Fig. 2) and each wheel has the same moment of inertia $I_w \triangleq I_{\mathrm{ws}_1}=I_{\mathrm{ws}_2}=I_{\mathrm{ws}_3}=I_{\mathrm{ws}_4}$, it can be shown that the momentum envelope with energy constraint E becomes an ellipsoid with the semi-axes of lengths $\sqrt{[4EI_w(1+\cos^2\theta)]}$, $\sqrt{[4EI_w(1+\cos^2\theta)]}$, and $\sqrt{[8EI_w]}\sin\theta$. (See Appendix B for the proof of this fact.) This provides a criterion for detecting whether the VSCMGs will encounter an inescapable singularity.

Theorem 1: Consider a VSCMG cluster used for attitude and power tracking. Assume that the VSCMG cluster has a pyramid configuration with angle θ and the wheels have the same moment of inertia I_w. Then, for a given energy command history $E(t)$ and angular momentum command history $\boldsymbol{H}(t)$ for $t_0\le t\le t_f$, the VSCMG cluster encounters an inescapable singularity, if and only if there exist $\bar{t}\in[t_0,t_f]$ such that

$$\frac{H_x^2(\bar{t})}{4E(\bar{t})I_{\mathrm{w}}(1+\cos^2\theta)}+\frac{H_y^2(\bar{t})}{4E(\bar{t})I_{\mathrm{w}}(1+\cos^2\theta)}+\frac{H_z^2(\bar{t})}{8E(\bar{t})I_{\mathrm{w}}\sin^2\theta}\geqslant 1 \tag{47}$$

where $H_x(\bar{t})$, $H_y(\bar{t})$, and $H_z(\bar{t})$ are the components of $\boldsymbol{H}(\bar{t})$ in the body frame.

Specifically, when the skew angle is $\theta=54.74$ deg, then $\cos\theta=1/\sqrt{3}$ and $\sin\theta=\sqrt{(2/3)}$ and the ellipsoid becomes a sphere with radius $\sqrt{[(16/3)E(\bar{t})I_w]}$. Therefore, the following is an immediate consequence of the theorem.

Corollary 1: Consider a VSCMG cluster used for attitude and power tracking. Assume that the VSCMG cluster has a regular pyramid configuration (skew angle $\theta=54.74$ deg) and the wheels have the same moment of inertia I_w. Then, for a given energy command history $E(t)$ and angular momentum command history $\boldsymbol{H}(t)$ for $t_0\le t\le t_f$, the VSCMG cluster encounters an inescapable singularity, if and only if there exist $\bar{t}\in[t_0,t_f]$ such that

$$\|\boldsymbol{H}(\bar{t})\|\geqslant\sqrt{(16/3)E(\bar{t})I_w} \tag{48}$$

One method to solve the inescapable singularity problem for VSCMGs for an IPACS is, therefore, to increase the workspace of the VSCMGs by increasing the inertia of the wheels as suggested by inequality (48). This means that the wheel size must be carefully determined depending on the spacecraft mission. Another possibility is to perform momentum dump/desaturation using external torque actuators such as magnetic torquers or gas thrusters. With this method, we can decrease $\|\boldsymbol{H}(t)\|$, thus keeping $\boldsymbol{H}(t)$ within the ellipsoid (or sphere) defined in the theorem (or corollary).

Once we know that the VSCMGs will never encounter inescapable singularities for a given attitude and power command from the theorem, we can apply the gradient method introduced in

Eqs. (24) and (25) by replacing Q with Q_p, that is,

$$\begin{bmatrix} \dot{\gamma} \\ \dot{\Omega} \end{bmatrix}_{\text{null}} = -k\left[\boldsymbol{I}_{2N} - \tilde{W}^{\frac{1}{2}}\left(Q_p \tilde{W}^{\frac{1}{2}}\right)^{\dagger} Q_p\right]\tilde{W} \begin{bmatrix} \dfrac{\partial \kappa}{\partial \gamma}^T \\ \dfrac{\partial \kappa}{\partial \Omega}^T \end{bmatrix} \tag{49}$$

where $A^{\dagger}$ denotes the Moore–Penrose inverse of the matrix A. The control law (49) will escape all singularities of the VSCMG system while tracking the required attitude and power reference commands.

IX. Numerical Examples

A numerical example is provided to test the proposed singularity avoidance method in Eq. (49). A spacecraft with four VSCMGs in a regular pyramid configuration is used for all numerical simulations. Table 1 contains the parameters used for the simulations. They closely parallel those used in Refs. 13, 15 and 18. In Table 1 ${}^{B}I$ is the spacecraft moment of inertia matrix without the VSCMG cluster and I_{g*}, $* = g, t$, and s, are the inertias of the gimbal frame. For more information on the exact equations on motion for a spacecraft with a VSCMG cluster, see Ref. 15.

Table 1 Simulation parameters

Parameter	Value
N	4
θ, deg	54.75
$\boldsymbol{\gamma}(0)$, rad	$[\pi/2, -\pi/2, -\pi/2, \pi/2]^T$
$\dot{\boldsymbol{\gamma}}(0)$, rad/s^2	$[0, 0, 0]^T$
${}^{B}I$, kg · m^2	$\begin{bmatrix} 15053 & 3000 & -1000 \\ 3000 & 6510 & 2000 \\ -1000 & 2000 & 11122 \end{bmatrix}$
I_{ws}, kg · m^2	diag{0.7, 0.7, 0.7, 0.7}
I_{wt}, I_{wg}, kg · m^2	diag{0.4, 0.4, 0.4, 0.4}
I_{gs}, I_{gt}, I_{gg}, kg · m^2	diag{0.1, 0.1, 0.1, 0.1}

The exact equations of motion from Ref. 15 are used in all simulations to validate our approach. For all simulations, the initial reference attitude is assumed to be aligned with the inertial frame, and the angular velocity of the reference attitude is chosen as

$$\boldsymbol{\omega}_{\text{d}}(t) = \begin{bmatrix} 2 \times 10^{-3} \sin(2\pi t/9000) \\ -3 \times 10^{-3} \sin(2\pi t/12000) \\ 1 \times 10^{-3} \sin(2\pi t/10000) \end{bmatrix} \text{(rad/s)}$$

The initial attitude of the spacecraft body frame is chosen as

$$\boldsymbol{q}_0 = [-1, 1, -1, 1]^T \big/ \sqrt{4} \tag{50}$$

where $\boldsymbol{q}$ is the Euler parameter vector with respect to the inertial frame. The initial attitude in Eq. (50) corresponds to the 3–2–1 Euler angle set $\phi_0 = -90$, $\theta_0 = 0$, and $\psi_0 = -90$ deg. The initial angular velocity of the body frame is set to zero.

The results from two simulation are presented. In the first case, only the attitude and power tracking control of Eq. (30) is applied. In the second case, the singularity avoidance control of Eq. (49) is

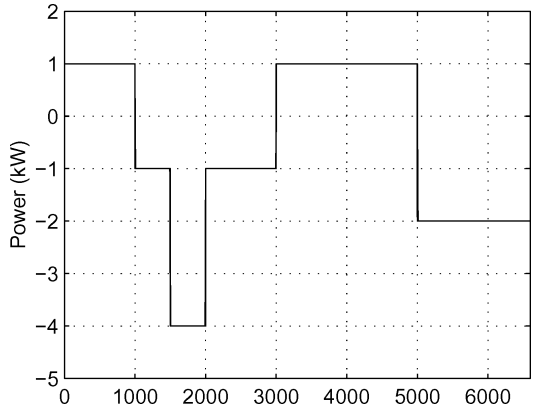

Fig. 9 Desired and actual power profile.

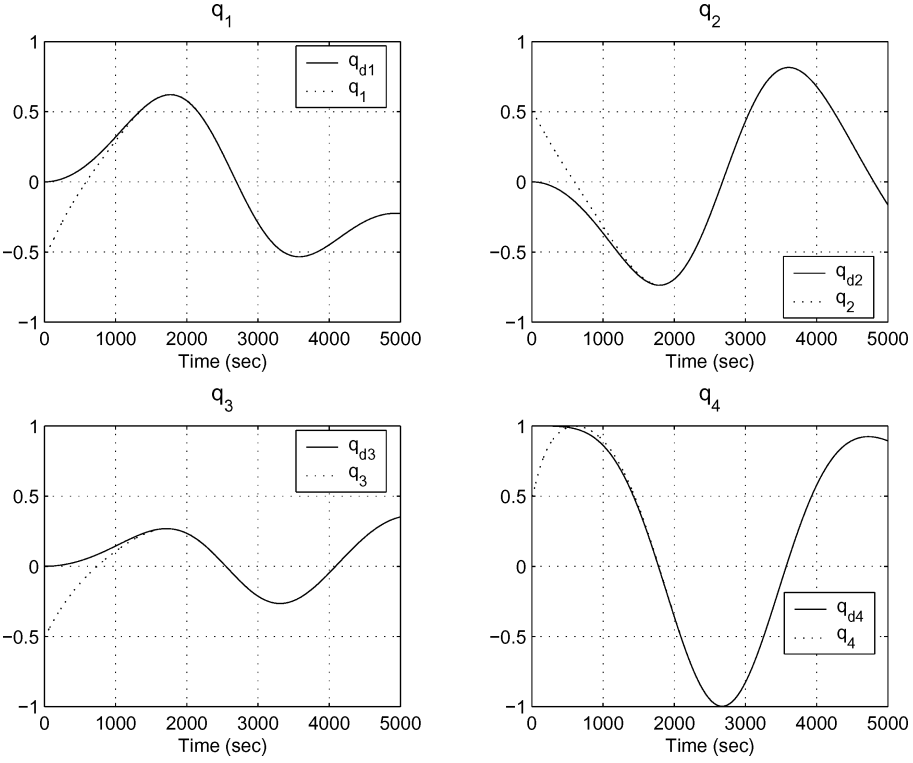

Fig. 8 Reference and actual attitude trajectory.

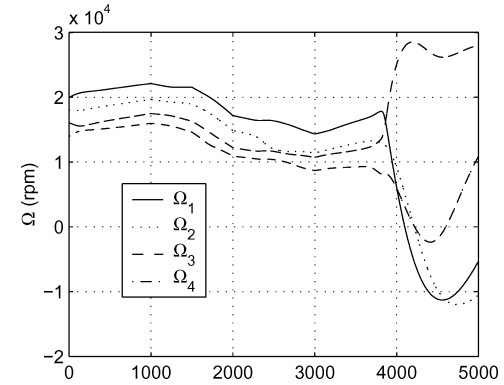

a) Angular speed of wheels

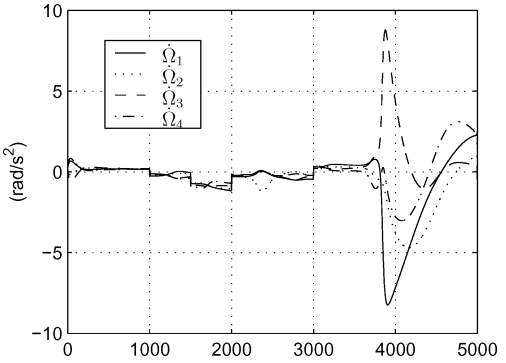

c) Wheel acceleration control input

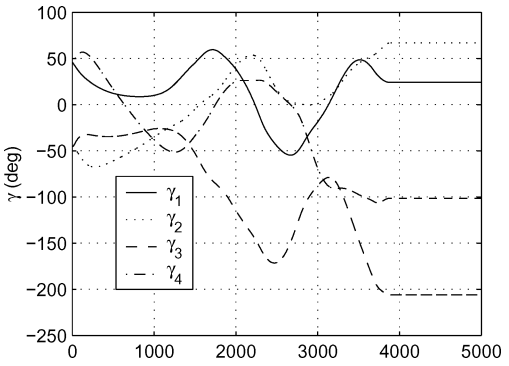

b) Gimbal angle

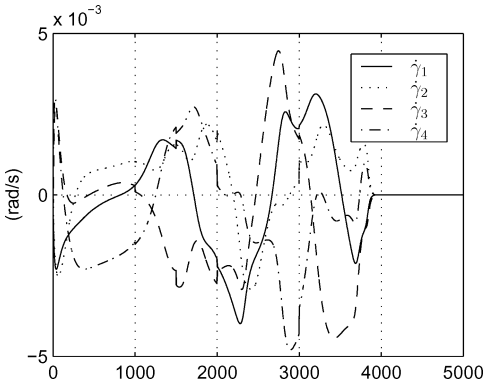

d) Gimbal rate control input

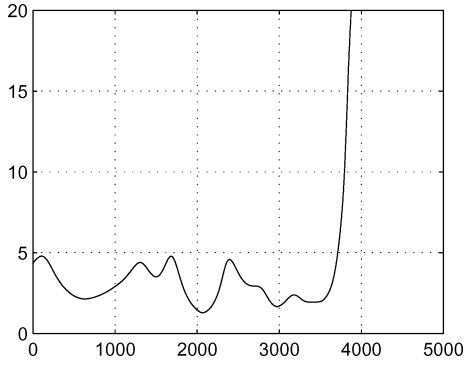

e) Condition number of C

Fig. 10 Simulation without singularity avoidance.

used in addition to Eq. (30). The gain in the singularity avoidance control is chosen as $k = 0.005$. Figure 8 shows the reference and actual attitude histories. In Figs. 8, the subscript d designates the desired quaternion history. The spacecraft attitude tracks the desired attitude exactly after a short period of time. The reference and the actual power profiles are shown in Fig. 9. The two profiles overlap each other perfectly and appear as a single line in Fig. 9. Figures 8 and 9 show that both attitude and power tracking are successfully achieved. Figure 10 shows that the matrix C becomes close to being singular at approximately $t = 4000$ s without any singularity avoidance algorithm. The control input $\dot{\boldsymbol{\Omega}}$ becomes very large during this period, becasue the weighting matrix W in Eq. (30) makes the VSCMGs operate in reaction wheel mode, and so $\dot{\boldsymbol{\Omega}}$ has to generate the required output torque. Note that without the weighting matrix, the gimbal rate input $\dot{\boldsymbol{\gamma}}$ would become very large, instead of $\dot{\boldsymbol{\Omega}}$. Both cases are undesirable.

On the other hand, Fig. 11 shows that singularities are successfully avoided using the null motion algorithm of Eq. (49). Although slightly larger control inputs $\dot{\boldsymbol{\gamma}}$ are needed to reconfigure the gimbal angles as the matrix C approach the singular states, the overall magnitudes of both $\dot{\boldsymbol{\gamma}}$ and $\dot{\boldsymbol{\Omega}}$ are kept within a reasonable range, contrary to the case without a singularity avoidance strategy. The attitude and power history profiles are exactly the same as the earlier case and are shown in Figs. 8 and 9. Note that the attitude and the power time histories with null motion are identical to those without null motion, that is, the null motion has affected neither the output torque nor the delivered power to the spacecraft bus, as expected.

Figure 12 shows that the singularity cannot be avoided even using the null motion method, if the criterion in the theorem is violated. In Fig. 12a, the magnitude of the total angular momentum $\|\boldsymbol{H}\|$ and the radius of the momentum envelope of the VSCMGs, which is equal to $\sqrt{[(16/3)EI_w]}$, are plotted. During the period when $\|\boldsymbol{H}(t)\| < \sqrt{[(16/3)E(t)I_w]}$, singularities are avoided using null motion, but when $\|\boldsymbol{H}(t)\| \approx \sqrt{[(16/3)E(t)I_w]}$ (near $t = 6600$s) the condition number $\kappa(\boldsymbol{\gamma}, \boldsymbol{\Omega})$ increases, as shown in Fig. 12b.

At this instant, the value of the matrix M defined in Eq. (36) is given by

$$M \approx \begin{bmatrix} 0.6844 & 0.6719 & 0.4073 & 0.4686 \\ \underline{0.6844} & \underline{0.6719} & \underline{0.4073} & \underline{0.4686} \\ 0.0011 & 0.0011 & 0.0011 & 0.0011 \end{bmatrix}$$

It can be seen that at this instant the row vectors of the matrix M are parallel to each other, as expected by the analysis in Sec. VII.

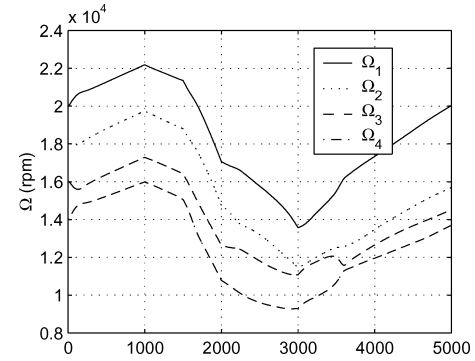

a) Angular speed of wheels

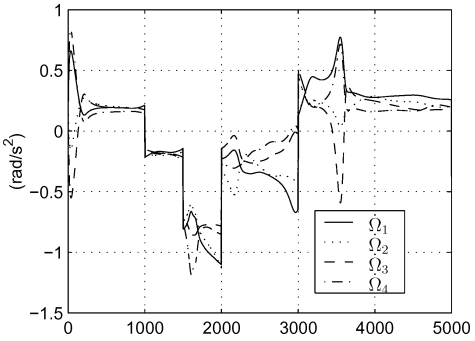

c) Wheel acceleration control input

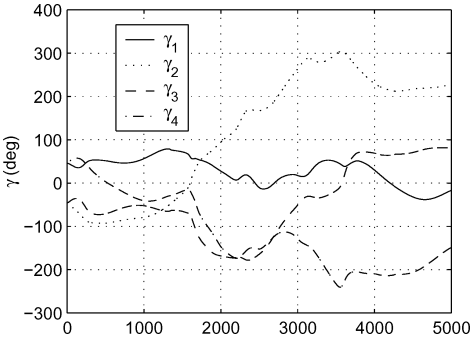

b) Gimbal angle

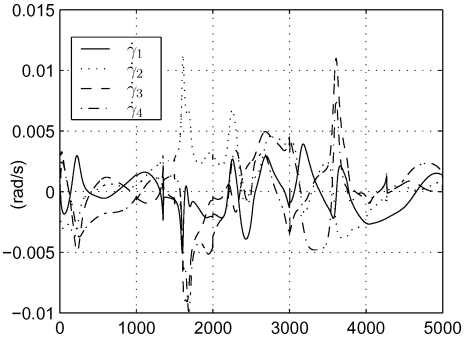

d) Gimbal rate control input

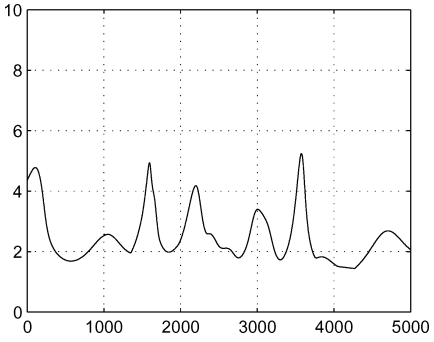

e) Condition number of C

Fig. 11 Simulation with singularity avoidance.

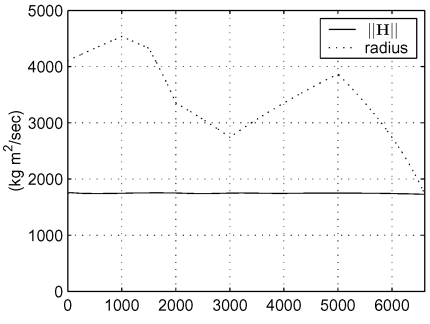

a) Norm of $H(t)$ and radius of momentum envelope

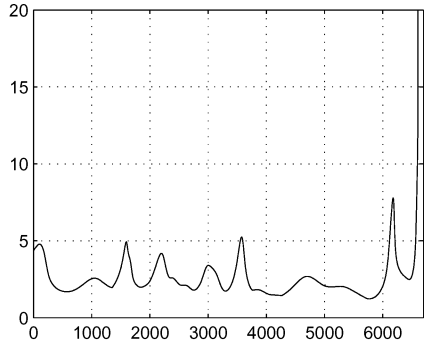

b) Condition number of C

Fig. 12 Inescapable singularity.

X. Conclusions

In this paper the properties of the singular states of a conventional CMG system are reviewed. Building on this, the singularity problem associated with a VSCMGs system is introduced and studied in detail. A VSCMG system has more degrees of freedom than a conventional CMG system, and so, in theory, it can generate arbitrary torques. However, in practice, it is still desirable to keep the gimbal angles away from singular configurations to make the best use of the torque amplification effect of the CMGs.

A gradient-based method using null motion has been introduced to avoid the singularities of a VSCMG cluster. It has been shown that this method will work if no less than two wheels operate in variable wheel speed mode and there is no power requirement. If a power trajectory command must also be tracked as in an IPACS, then the VSCMG system may encounter inescapable singularities.

We have shown that all such inescapable singularities are external, that is, they all lie on the momentum envelope subject to the kinetic energy constraint of the VSCMGs. Geometric and algebraic considerations provide a criterion for determining whether the VSCMGs will encounter an inescapable singularity. This criterion can be used to determine the size of a VSCMG system for a given attitude/power mission.

Appendix A: Solution of Optimization Problem VII.A.

To show solution (44) let $\phi_i \in [0, \pi/2]$ denote the angle between $\boldsymbol{u}$ and $\boldsymbol{s}_i$ at the singular configuration with $\epsilon_i = \text{sign}(\boldsymbol{s}_i \cdot \boldsymbol{u}) = +1$ in Fig. 3. The value of $\alpha_i \triangleq \boldsymbol{u} \cdot \boldsymbol{s}_i$ is maximum at this singular configuration, and so we have that

$$\alpha_{\max i} = \max\{\boldsymbol{u} \cdot \boldsymbol{s}_i\} = \cos\phi_i = \sqrt{1 - \sin^2(\phi_i)}$$
$$= \sqrt{1 - \cos^2(\pi - \phi_i)} = \sqrt{1 - (\boldsymbol{g}_i \cdot \boldsymbol{u})^2}$$

Introduce the Lagrange multipliers λ_0 and λ_i for $i = 1, \ldots, N$ and define the Lagrangian $\mathcal{L}$ as

$$\mathcal{L} \triangleq \sum_{i=1}^{N} \alpha_i I_{\text{ws}_i} \Omega_i - \lambda_0 \left(\sum_{i=1}^{N} I_{\text{ws}_i} \Omega_i^2 - 2E \right) - \sum_{i=1}^{N} \lambda_i \left(\alpha_i^2 - \alpha_{\max_i}^2 \right)$$

Then the necessary conditions for a maximum are

$$\frac{\partial \mathcal{L}}{\partial \Omega_i} = \alpha_i^* I_{\text{ws}_i} - 2\lambda_0^* I_{\text{ws}_i} \Omega_i^* = 0, \qquad i = 1, \ldots, N \quad \text{(A1)}$$

$$\frac{\partial \mathcal{L}}{\partial \alpha_i} = I_{\text{ws}_i} \Omega_i^* - 2\lambda_i^* \alpha_i^* = 0, \qquad i = 1, \ldots, N \quad \text{(A2)}$$

The complementary slackness conditions

$$\lambda_i^* \left(\alpha_i^{*2} - \alpha_{\max_i}^2 \right) = 0, \qquad i = 1, \ldots, N \quad \text{(A3)}$$

also must be satisfied.

If $\lambda_0^* = 0$ then Eq. (A1) implies that $\alpha_i^* = 0$ for all $i = 1, \ldots, N$ and Eq. (A2) yields that $\Omega_i^* = 0$ for all $i = 1, \ldots, N$, which violates the energy constraint. Hence, $\lambda_0^* \neq 0$, and thus, Eq. (A1) yields that

$$\Omega_i^* = \alpha_i^* \big/ 2\lambda_0^*, \qquad i = 1, \ldots, N \quad \text{(A4)}$$

Now, let us show that the maximizing solution satisfies $\lambda_i^* \neq 0$ for all $i = 1, \ldots, N$. To this end assume that an optimal solution exists such that $\lambda_k^* = 0$ for some $k \in \{1, \ldots, N\}$. It follows from Eq. (A2) that $\Omega_k^* = 0$. Clearly, there exists at least one wheel with nonzero wheel speed, to satisfy the energy constraint. Without loss of generality, let this be the $(k+1)$th wheel. Then, we have $\lambda_k^* = \Omega_k^* = 0$ and $\lambda_{k+1}^* \neq 0$ and $\Omega_{k+1}^* \neq 0$. To satisfy the energy constraint,

$$I_{\text{ws}_{k+1}} \Omega_{k+1}^{*2} = 2E - \sum_{\substack{i=1 \\ i \neq k, k+1}}^{N} I_{\text{ws}_i} \Omega_i^{*2} \triangleq 2E'$$

and from Eq. (A3), $\alpha_{k+1}^* = \alpha_{\max_{k+1}}$ because $\alpha_{k+1}^* = -\alpha_{\max_{k+1}}$ is not the maximum obviously.

Let now $\Omega_i^{**} = \Omega_i^*$, $\alpha_i^{**} = \alpha_i^*$ for $i = 1, \ldots, k-1, k+2, \ldots, N$ and let

$$\Omega_i^{**} = \alpha_{\max_i} \big/ 2\lambda_0^{**}, \qquad \alpha_i^{**} = \alpha_{\max_i}, \qquad i = k,\ k+1$$

where

$$\lambda_0^{**} = 1 \big/ \sqrt{8E'} \left(I_{\text{ws}_k} \alpha_{\max_k}^2 + I_{\text{ws}_{k+1}} \alpha_{\max_{k+1}}^2 \right)^{\frac{1}{2}}$$

It is easily shown that this solution satisfies the constraints (42) and (43).

The cost of the solution (α_i^*, Ω_i^*) is given by

$$\mathcal{J}^* = \sum_{i=1}^{N} \alpha_i^* I_{\text{ws}_i} \Omega_i^* = \sum_{\substack{i=1 \\ i \neq k, k+1}}^{N} \alpha_i^* I_{\text{ws}_i} \Omega_i^* + \alpha_{k+1}^* I_{\text{ws}_{k+1}} \Omega_{k+1}^*$$

$$= \sum_{\substack{i=1 \\ i \neq k, k+1}}^{N} \alpha_i^* I_{\text{ws}_i} \Omega_i^* + \sqrt{2E' I_{\text{ws}_{k+1}} \alpha_{\max_{k+1}}^2} \quad \text{(A5)}$$

whereas the cost for the solution $(\alpha_i^{**}, \Omega_i^{**})$ is given by

$$\mathcal{J}^{**} = \sum_{i=1}^{N} \alpha_i^{**} I_{\text{ws}_i} \Omega_i^{**}$$

$$= \sum_{\substack{i=1 \\ i \neq k, k+1}}^{N} \alpha_i^* I_{\text{ws}_i} \Omega_i^* + \alpha_k^{**} I_{\text{ws}_k} \Omega_k^{**} + \alpha_{k+1}^{**} I_{\text{ws}_{k+1}} \Omega_{k+1}^{**}$$

$$= \sum_{\substack{i=1 \\ i \neq k, k+1}}^{N} \alpha_i^* I_{\text{ws}_i} \Omega_i^* + \sqrt{2E' \left(I_{\text{ws}_k} \alpha_{\max_k}^2 + I_{\text{ws}_{k+1}} \alpha_{\max_{k+1}}^2 \right)} \quad \text{(A6)}$$

Clearly, $\mathcal{J}^* \leq \mathcal{J}^{**}$. Moreover, $\mathcal{J}^* = \mathcal{J}^{**}$ if and only if $\alpha_{\max_k} = 0$, that is, when $\boldsymbol{u} = \pm \boldsymbol{g}_k$. However, in this case $\Omega_k^* = 0$ regardless of the value of λ_k^*. It follows that at the maximizing solution $\lambda_i^* \neq 0$ for all $i = 1, \ldots, N$.

When the fact that $\lambda_i^* \neq 0$ for all $i = 1, \ldots, N$, is used, the complementary slackness condition (A3) yields that

$$\alpha_i^* = \alpha_{\max_i}, \qquad i = 1, \ldots, N$$

and from Eq. (A4),

$$\Omega_i^* = \alpha_{\max_i}^* \big/ 2\lambda_0^*, \qquad i = 1, \ldots, N$$

Moreover, to satisfy the energy constraint,

$$\sum_{i=1}^{N} I_{\text{ws}_i} \Omega_i^{*2} = \frac{\sum_{i=1}^{N} I_{\text{ws}_i} \alpha_{\max_i}^2}{4\lambda_0^{*2}} = 2E$$

Thus, we have

$$\lambda_0^* = \frac{1}{\sqrt{8E}} \left(\sum_{i=1}^{N} I_{\text{ws}_i} \alpha_{\max_i}^2 \right)^{\frac{1}{2}}$$

which completes the proof.

Next, we show that the maximizer (44) occurs if and only if the VSCMG system encounters a singularity such that rank $M = 1$, where M is given in Eq. (36), that is, an inescapable singularity.

Sufficiency follows from the fact that $\alpha_i^* = \alpha_{\max_i}$ implies a singularity with $\epsilon_i = +1$ for all $i = 1, \ldots, N$. Then the matrix M defined in Eq. (36) becomes

$$M = \begin{bmatrix} I_{\text{ws}_1} \boldsymbol{u} \cdot \boldsymbol{s}_1 & I_{\text{ws}_2} \boldsymbol{u} \cdot \boldsymbol{s}_2 & \ldots & I_{\text{ws}_N} \boldsymbol{u} \cdot \boldsymbol{s}_N \\ I_{\text{ws}_1} \Omega_1^* & I_{\text{ws}_2} \Omega_2^* & \ldots & I_{\text{ws}_N} \Omega_N^* \end{bmatrix}$$

$$= \begin{bmatrix} I_{\text{ws}_1} \alpha_{\max_1} & \ldots & I_{\text{ws}_N} \alpha_{\max_N} \\ I_{\text{ws}_1} \alpha_{\max_1} \big/ 2\lambda_0^* & \ldots & I_{\text{ws}_N} \alpha_{\max_N} \big/ 2\lambda_0^* \end{bmatrix}$$

which obviously has rank 1.

To show necessity, notice that when the VSCMG system encounters a singularity with rank $M = 1$, then necessarily $\epsilon_i = \text{sign}(\boldsymbol{u} \cdot \boldsymbol{s}_i) = +1$ for all $i = 1, \ldots, N$, and thus, $\alpha_i = \alpha_{\max i}$, $i = 1, \ldots, N$. Moreover, there exists a constant $\eta > 0$ such that $\boldsymbol{\Omega}^T = \eta[\boldsymbol{u} \cdot \boldsymbol{s}_1, \ldots, \boldsymbol{u} \cdot \boldsymbol{s}_N]$. The energy constraint must be satisfied, that is,

$$E = \tfrac{1}{2} \boldsymbol{\Omega}^T I_{\text{ws}} \boldsymbol{\Omega} = \tfrac{1}{2} \eta^2 \sum_{i=1}^{N} I_{\text{ws}i} (\boldsymbol{u} \cdot \boldsymbol{s}_i)^2 = \tfrac{1}{2} \eta^2 \sum_{i=1}^{N} I_{\text{ws}_i} \alpha_{\max_i}^2$$

thus,

$$\eta = \sqrt{\frac{2E}{\sum_{i=1}^{N} I_{\mathrm{ws}_i} \alpha_{\max_i}^2}} = \frac{1}{2\lambda_0^*}$$

which implies that

$$\Omega_i^* = \frac{\alpha_{\max_i}}{2\lambda_0^*}, \qquad i = 1, \ldots, N$$

thus completing the proof.

Appendix B: Momentum Envelope for Given Energy

Let $c_\theta \triangleq \cos\theta$ and $\mathrm{s}_\theta \triangleq \sin\theta$. Then the gimbal axes of the VSCMG system in Fig. 2 with skew angle θ are

$$\boldsymbol{g}_1 = [s_\theta, 0, c_\theta]^T, \qquad \boldsymbol{g}_2 = [0, s_\theta, c_\theta]^T$$

$$\boldsymbol{g}_3 = [-s_\theta, 0, c_\theta]^T, \qquad \boldsymbol{g}_4 = [0, -s_\theta, c_\theta]^T$$

Also assume that every wheel has the same moment of inertia I_w, that is, $I_{\mathrm{ws}_i} = I_w$ for all $i = 1, \ldots, N$. Then, for an arbitrary singular direction vector $\boldsymbol{u} = [u_1, u_2, u_3]^T$, and using Eq. (45), the total angular momentum vector becomes

$$\boldsymbol{H} = \frac{I_w}{2\lambda_0^*}\left[4\boldsymbol{u} - \sum_{i=1}^{4} \boldsymbol{g}_i(\boldsymbol{g}_i \cdot \boldsymbol{u})\right] = \frac{I_w}{\lambda_0^*}\begin{bmatrix} \left(1 + c_\theta^2\right)u_1 \\ \left(1 + c_\theta^2\right)u_1 \\ 2s_\theta^2 u_3 \end{bmatrix}$$

We also have

$$\boldsymbol{H} \cdot \boldsymbol{u} = \frac{I_w}{2\lambda_0^*}\left[4 - \sum_{i=1}^{4} (\boldsymbol{g}_i \cdot \boldsymbol{u})^2\right]$$

Since

$$\lambda_0^{*2} = \frac{I_w}{8E}\sum_{i=1}^{4} \alpha_{\max_i}^2 = \frac{I_w}{8E}\left[4 - \sum_{i=1}^{4} (\boldsymbol{g}_i \cdot \boldsymbol{u})^2\right] = \frac{\lambda_0^*}{4E}\boldsymbol{H} \cdot \boldsymbol{u}$$

it follows that

$$\lambda_0^* = (\boldsymbol{H} \cdot \boldsymbol{u})/4E$$

Therefore,

$$(\boldsymbol{H} \cdot \boldsymbol{u})\boldsymbol{H} = 4E I_w A\boldsymbol{u}$$

where $A \triangleq \mathrm{diag}\{1 + c_\theta^2, 1 + \mathrm{c}_\theta^2, 2s_\theta^2\}$, which implies

$$\boldsymbol{u} = [(\boldsymbol{H} \cdot \boldsymbol{u})/4E I_w]A^{-1}\boldsymbol{H}$$

Finally, taking the dot product with $\boldsymbol{H}$ in both sides yields

$$\boldsymbol{H} \cdot \boldsymbol{u} = [(\boldsymbol{H} \cdot \boldsymbol{u})/4E I_{\mathrm{sw}}]\boldsymbol{H}^T A^{-1}\boldsymbol{H}$$

Therefore, we have the following quadratic equation for all possible values of $\boldsymbol{H}$

$$\boldsymbol{H}^T B\boldsymbol{H} = 1 \tag{B1}$$

where

$$B \triangleq \frac{1}{4E I_w}A^{-1} = \begin{bmatrix} \dfrac{1}{4E I_w\left(1 + c_\theta^2\right)} & 0 & 0 \\ 0 & \dfrac{1}{4E I_w\left(1 + c_\theta^2\right)} & 0 \\ 0 & 0 & \dfrac{1}{8E I_w s_\theta{}^2} \end{bmatrix}$$

The last equation represents an ellipsoid with the semiaxes of lengths $\sqrt{[4E I_w(1 + \cos^2\theta)]}$, $\sqrt{[4E I_w(1 + \cos^2\theta)]}$, and $\sqrt{(8E I_w)}\sin\theta$.

Acknowledgments

Support for this work has been provided through the Air Force Office of Scientific Research/ Air Force Research Laboratory award F49620-00-1-0374. The authors acknowledge helpful discussions with H. Kurokawa and B. Wie concerning the control moment gyro singularity problem.

References

[1]Margulies, G., and Aubrun, J. N., "Geometric Theory of Single-Gimbal Control Moment Gyro Systems," *Journal of the Astronautical Science*, Vol. 26, No. 2, 1978, pp. 159–191.

[2]Cornick, D. E., "Singularity Avoidance Control Laws for Single Gimbal Control Moment Gyros," *AIAA Guidance and Control Conference*, AIAA, New York, 1979, pp. 20–33.

[3]Tokar, E. N., and Platonov, V. N., "Singular Surfaces in Unsupported Gyrodyne Systems," *Cosmic Research*, Vol. 16, No. 5, 1979, pp. 547–555.

[4]Kurokawa, H., "A Geometry Study of Single Gimbal Control Moment Gyros—Singularity Problem and Steering Law," TR 175, Mechanical Engineering Lab., Tsukuba, Japan, Jan. 1998.

[5]Oh, H., and Vadali, S., "Feedback Control and Steering Laws for Spacecraft Using Single Gimbal Control Moment Gyro," *Journal of the Astronautical Sciences*, Vol. 39, No. 2, 1991, pp. 183–203.

[6]Ford, K. A., and Hall, C. D., "Singular Direction Avoidance Steering for Control-Moment Gyros," *Journal of Guidance, Control, and Dynamics*, Vol. 23, No. 4, 2000, pp. 648–656.

[7]Wie, B., Bailey, D., and Heiberg, C. J., "Singularity Robust Steering Logic for Redundant Single-Gimbal Control Moment Gyros," *Journal of Guidance, Control, and Dynamics*, Vol. 24, No. 5, 2001, pp. 865–872.

[8]Wie, B., "New Singularity Escape and Avoidance Steering Logic for Control Moment Gyro Systems," AIAA Paper 2003-5659, Aug. 2003.

[9]Paradiso, J. A., "Global Steering of Single Gimballed Control Moment Gyroscopes Using a Directed Search," *Journal of Guidance, Control, and Dynamics*, Vol. 15, No. 5, 1992, pp. 1236–1244.

[10]Vadali, S. R., Oh, H. S., and Walker, S. R., "Preferred Gimbal Angles for Single Gimbal Control Moment Gyros," *Journal of Guidance Control, and Dynamics*, Vol. 13, No. 6, 1990, pp. 1090–1095.

[11]Kurokawa, H., "Constrained Steering Law of Pyramid-Type Control Moment Gyros and Ground Tests," *Journal of Guidance, Control, and Dynamics*, Vol. 20, No. 3, 1997, pp. 445–449.

[12]Ford, K. A., and Hall, C. D., "Flexible Spacecraft Reorientations Using Gimbaled Momentum Wheels," *Advances in the Astronautical Sciences, Astrodynamics*, edited by F. Hoots, B. Kaufman, P. J. Cefola, and D. B. Spencer, Vol. 97, Univelt, San Diego, CA, 1997, pp. 1895–1914.

[13]Schaub, H., Vadali, S. R., and Junkins, J. L., "Feedback Control Law for Variable Speed Control Moment Gyroscopes," *Journal of the Astronautical Sciences*, Vol. 46, No. 3, 1998, pp. 307–328.

[14]Tsiotras, P., Shen, H., and Hall, C., "Satellite Attitude Control and Power Tracking with Energy/Momentum Wheels," *Journal of Guidance, Control, and Dynamics*, Vol. 24, No. 1, 2001, pp. 23–34.

[15]Yoon, H., and Tsiotras, P., "Spacecraft Adaptive Attitude and Power Tracking With Variable Speed Control Moment Gyroscopes," *Journal of Guidance, Control, and Dynamics*, Vol. 25, No. 6, 2002, pp. 1081–1090.

[16]Roes, J. B., "An Electro-Mechanical Energy Storage System for Space Application," *Progress in Astronautics and Rocketry*," Vol. 3, Academic Press, New York, 1961, pp. 613–622.

[17]Hall, C. D., "High-Speed Flywheels for Integrated Energy Storage and Attitude Control," *American Control Conference*, American Automatic Control Council, Evanston, IL, 1997, pp. 1894–1898.

[18]Richie, D. J., Tsiotras, P., and Fausz, J. L., "Simultaneous Attitude Control and Energy Storage using VSCMGs : Theory and Simulation," *American Control Conference*, American Automatic Control Council, Evanston, IL, 2001, pp. 3973–3979.

[19]Wie, B., "Singularity Analysis and Visualization for Single-Gimbal Control Moment Gyro Systems," AIAA Paper 2003-5658, Aug. 2003.

[20]Schaub, H., and Junkins, J. L., "Singularity Avoidance Using Null Motion and Variable-Speed Control Moment Gyros," *Journal of Guidance Control, and Dynamics*, Vol. 23, No. 1, 2000, pp. 11–16.

[21]Bedrossian, N. S., Paradiso, J., Bergmann, E. V., and Rowell, D., "Redundant Single Gimbal Control Moment Gyroscope Singularity Analysis," *Journal of Guidance, Control, and Dynamics*, Vol. 13, No. 6, 1990, pp. 1096–1101.

[22]Bedrossian, N. S., Paradiso, J., Bergmann, E. V., and Rowell, D., "Steering Law Design for Redundant Single-Gimbal Control Moment Gyroscopes," *Journal of Guidance, Control, and Dynamics*, Vol. 13, No. 6, 1990, pp. 1083–1089.

[23]Horn, R., and Johnson, C. R., *Matrix Analysis*, Cambridge Univ. Press, Cambridge, England, U.K., 1985, pp. 427, 449.

[24]Junkins, J. L., and Kim, Y., *Introduction to Dynamics and Control of Flexible Structures*, AIAA, Washington, DC, 1993, pp. 48, 49.